

*g*

2

AD A 053588

**DIGITAL SIMULATION OF FLEXIBLE AIRCRAFT  
RESPONSE TO SYMMETRICAL AND ASYMMETRICAL  
RUNWAY ROUGHNESS**

Anthony G. Gerardi

Structural Integrity Branch  
Structural Mechanics Division

August 1977

TECHNICAL REPORT AFFDL-TR-77-37

DDC FILE COPY

Approved for public release; distribution unlimited.

AIR FORCE FLIGHT DYNAMICS LABORATORY  
AIR FORCE WRIGHT AERONAUTICAL LABORATORIES  
AIR FORCE SYSTEMS COMMAND  
WRIGHT-PATTERSON AIR FORCE BASE, OHIO 45433

DDC  
RECEIVED  
MAY 3 1978  
B

*g*

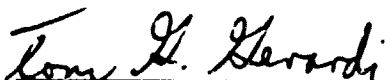
**Best  
Available  
Copy**

NOTICE

When Government drawings, specifications, or other data are used for any purpose other than in connection with a definitely related Government procurement operation, the United States Government thereby incurs no responsibility nor any obligation whatsoever; and the fact that the government may have formulated, furnished, or in any way supplied the said drawings, specifications, or other data, is not to be regarded by implication or otherwise as in any manner licensing the holder or any other person or corporation, or conveying any rights or permission to manufacture, use, or sell any patented invention that may in any way be related thereto.

This report has been reviewed by the Information Office (IO) and is releasable to the National Technical Information Service (NTIS). At NTIS, it will be available to the general public, including foreign nations.

This technical report has been reviewed and is approved for publication.

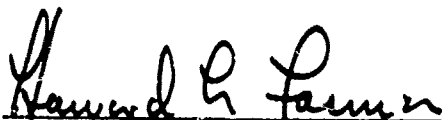


TONY G. GERARDI  
Project Engineer

FOR THE COMMANDER



ROBERT M. BADER, Chief  
Structural Integrity Branch  
Structural Mechanics Division



HOWARD L. FARMER, COL, USAF  
Chief, Structural Mechanics Division

Copies of this report should not be returned unless return is required by security considerations, contractual obligations, or notice on a specific document.

UNCLASSIFIED

SECURITY CLASSIFICATION OF THIS PAGE (When Data Entered)

<b>REPORT DOCUMENTATION PAGE</b>		READ INSTRUCTIONS BEFORE COMPLETING FORM	
1. REPORT NUMBER <b>AFFDL-TR-77-37</b>		2. GOVT ACCESSION NO.	
3. TITLE (and Subtitle) <b>DIGITAL SIMULATION OF FLEXIBLE AIRCRAFT RESPONSE TO SYMMETRICAL AND ASYMMETRICAL RUNWAY ROUGHNESS</b>		4. PERFORMING ORG. REPORT NUMBER <b>Final Technical Report, Sept 1975 - Aug 1976</b>	
5. AUTHOR <b>Anthony G. Gerardi</b>		6. CONTRACT OR GRANT NUMBER(s)	
7. PERFORMING ORGANIZATION NAME AND ADDRESS Air Force Flight Dynamics Laboratory Structural Integrity Branch Wright-Patterson AFB, Ohio 45433		8. PROJECT OR TASK NUMBER Project No. 1367 Task No. 136701 Work Unit No. 13670113	
9. CONTROLLING OFFICE NAME AND ADDRESS Air Force Flight Dynamics Laboratory Air Force Systems Command Wright-Patterson AFB, Ohio 45433		10. SECURITY CLASS (of this Report) <b>UNCLASSIFIED</b>	
11. MONITORING AGENCY NAME & ADDRESS (if different from Controlling Office)		12. NUMBER OF PAGES 83	
13. DISTRIBUTION STATEMENT (of this Report) Approved for public release; distribution unlimited			
14. DISTRIBUTION STATEMENT (of the abstract entered in Block 20, if different from Report)			
15. SUPPLEMENTARY NOTES			
16. KEY WORDS (Continue on reverse side if necessary and identify by block number) Aircraft Dynamics Simulation Ground Loads Taxi Analysis			
17. ABSTRACT (Continue on reverse side if necessary and identify by block number) A method has been developed for determining the dynamic response of a flexible aircraft to runway roughness during takeoff or constant speed taxi. The equations that formulate the mathematical model have been programmed for a CDC 6600 digital computer and uses a Calcomp plotter for part of the program output. Three sets of runway elevation data are input to provide a forcing function at each landing gear. Three runway profiles measured at Washington National Airport, runway 36, were used to represent a typical commercial (OVER)			

6

10

9

16

17

11

12

83 p1

UNCLASSIFIED

SECURITY CLASSIFICATION OF THIS PAGE (When Data Entered)

1012070

at

UNCLASSIFIED

SECURITY CLASSIFICATION OF THIS PAGE(When Data Entered)

Block No. 20 - Continued

asymmetric profile. Three lines of profile were analytically generated to represent traversing a 1-cos dip at a 45 degree angle of approach.

Several aircraft have been simulated with this program, each during a takeoff and a constant speed taxi. The data used to simulate the airplanes (McDonnell Douglas C-9A, Boeing 727-100, and an AMST) and the runway profile data used, are included in the appendix of this paper.

Comparison of simulated results to limited experimental data was good. Peak vertical acceleration levels at the pilot's station were within 14%.

The effect of the asymmetry of a profile on pilot's station vertical acceleration was significant providing the asymmetry of the profile was significant.

UNCLASSIFIED

SECURITY CLASSIFICATION OF THIS PAGE(When Data Entered)

FOREWORD

This report was prepared by A. G. Gerardi, Aerospace Engineer in the Loads and Response Prediction Group of the Structural Mechanics Division of the Air Force Flight Dynamics Laboratory at Wright-Patterson Air Force Base, Ohio. The work described herein is a part of the Air Force Systems Command exploratory development program to predict aircraft dynamic loads during ground operations. The work was directed under Project 1367, "Structural Integrity for Military Aerospace Vehicles," Task 136701, "Structural Flight Loads Data."

This report covers work done in the period from September 1975 to August 1976.

ACCESSION for		
NTIS	White Section	<input checked="" type="checkbox"/>
DOC	Buff Section	<input type="checkbox"/>
UNANNOUNCED		<input type="checkbox"/>
JUSTIFICATION _____		
BY _____		
DISTRIBUTION/PRIORITY CODES		
Dist.	AVAIL	and/or SPECIAL
A		

## TABLE OF CONTENTS

Section	Page
I INTRODUCTION	1
1. Purpose of the Study	1
II MATHEMATICAL MODEL	3
1. General Airplane/Runway Model	3
2. Rigid Body Equations of Motion	6
3. Flexibility Equations of Motion	7
4. Solution Technique	7
III COMPUTER PROGRAM	9
1. Output Format	9
IV DISCUSSION OF SIMULATIONS	20
V SUMMARY AND CONCLUSIONS	38
APPENDIX	
A DEVELOPMENT OF EQUATIONS OF MOTION	41
B LISTING OF COMPUTER PROGRAM TAX2	48
C LISTING OF AIRPLANE DATA	62
D LISTING OF RUNWAY PROFILE DATA	71
BIBLIOGRAPHY	74
REFERENCES	75

## LIST OF ILLUSTRATIONS

Figure	Page
1. Accepted Military Human Tolerance Vertical Vibration Criterion	2
2. Typical Single Acting Oleo Pneumatic Landing Gear Strut	4
3. Source Deck Setup	16
4. Typical Calcomp Plotted Output	18
5. Boeing 727-100 Constant Speed Taxi Simulation over the Washington National Profile Without a Roll Degree of Freedom	22
6. Boeing 727-100 Constant Speed Taxi Simulation over the Washington National Profile With a Roll Degree of Freedom	23
7. PSD of Washington National Airport Runway 36	24
8. Boeing 727-100 Traversing a (1-cos) dip head-on	25
9. Boeing 727-100 Traversing a (1-cos) dip at a 45° angle	26
10. C-9A Traversing a (1-cos) dip at a 45° angle	28
11. AMST Traversing a (1-cos) dip at a 45° angle	29
12. Boeing 727-100 Taking Off from Washington National Airport With the Roll Degree of Freedom Included	30
13. AMST Taking Off from Washington National Airport With the Roll Degree of Freedom Included	31
14. C-9A Taking Off from Washington National Airport With the Roll Degree of Freedom Included	32
15. PSD of Washington National Runway 36 and two Typically Smooth Runways	33
16. Measured Response of a Boeing 727-100 Takeoff at Washington National Airport Runway 36	34
17. C-9A with Flexible Wings Taxiing over a (1-cos) dip at a 45° angle	36



LIST OF ILLUSTRATIONS (Continued)

Figure		Page
18.	C-9A with Flexible Wings Taking Off from Washington National Runway 36	37
A-1.	Description of Asymmetrical Mathematical Model	42
C-1.	Three View of Boeing 727-100	63
C-2.	Three View of McDonnell-Douglas C-9A	66
D-1.	Washington National Runway 36 with Linear Trend Removed	72

LIST OF TABLES

Table		Page
1	Description of Input Aircraft Data	10
2	Typical Computer Output Listing	17
3	Summary of Simulations	21
	Comparisons of Simulated and Experimental Data	35

SECTION I  
INTRODUCTION

A common problem that can occur during takeoff and taxiing operations of aircraft is high acceleration levels caused by a rough runway. Due to these accelerations, runway must be evaluated with respect to roughness in order to ensure timely pavement maintenance to control aircraft structural loads and fatigue. Also, rough runways adversely affect the ability of the crew members by reducing instrument readability and crew comfort. Figure 1 shows the current criterion (Reference 1) used to set maximum allowable vertical acceleration levels from a human comfort standpoint. Reference 2 addressed the runway roughness problem at considerable length and contains the development of a mathematical model and subsequent computer program called "TAXI" to simulate the dynamic response of military aircraft to runway roughness on a symmetrical runway. For a symmetric runway, only one runway profile is required. Normally this is sufficient for representing a paved runway. With the advent of the AMST (Advanced Medium STOL Transport) and in some cases with conventional airplanes operating off of semiprepared or very rough paved surfaces, the rolling motion of an aircraft became significant. This rolling motion was the result of operating the aircraft on an asymmetric runway. Therefore, in order to properly simulate this response it became necessary to include the runway profile encountered by each landing gear.

1. PURPOSE OF THIS STUDY

The purpose of this study is to develop a computer program, capable of simulating an aircraft during constant speed taxi or takeoff from runways that are asymmetrical.

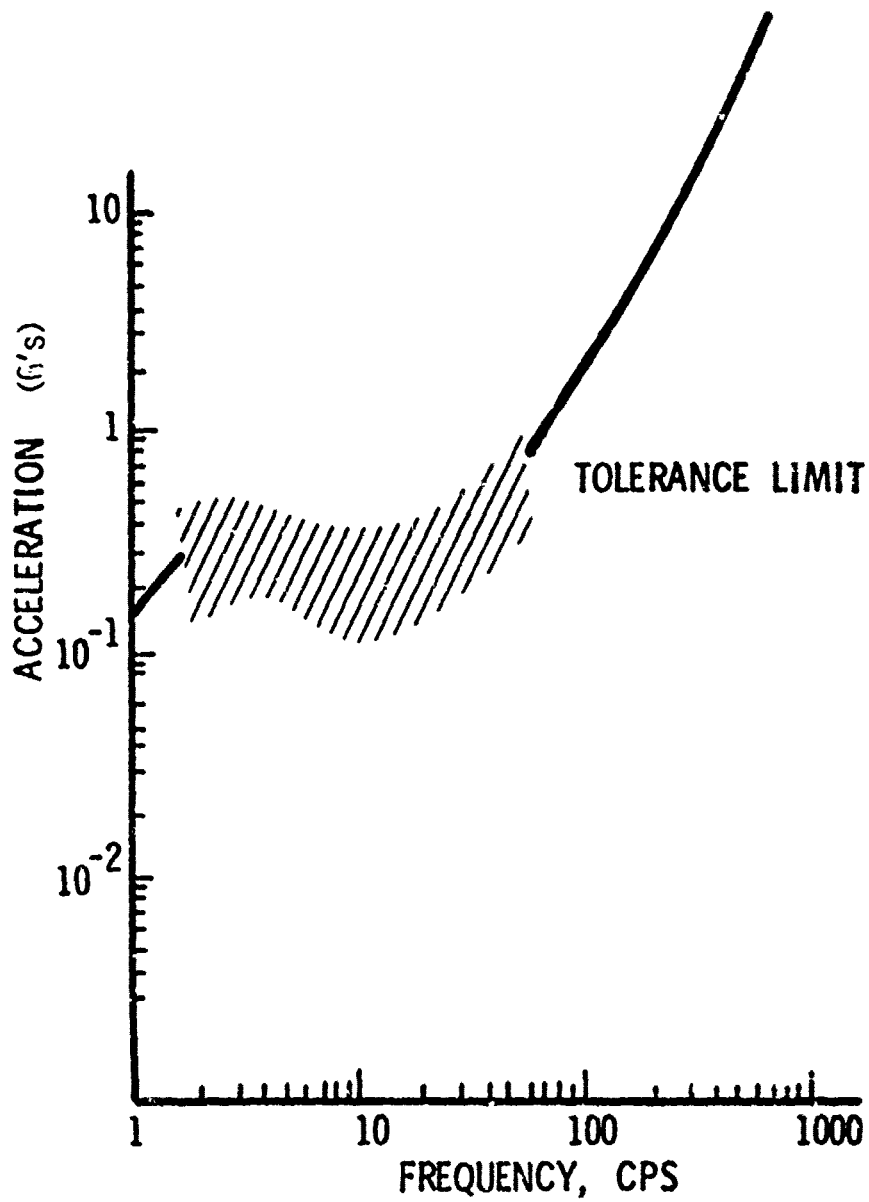


Figure 1. Accepted Military Human Tolerance Vertical Vibration Criterion

## SECTION II MATHEMATICAL MODEL

The airplane/runway mathematical model used for this study was the basic mathematical model developed in Reference 2. A detailed description of the components that make up this general model, as well as the assumptions made are shown in Reference 2. This report presents, in summary form, the landing gear strut and tire representation, the airplane rigid body and flexible body representation, the runway profile representation, the equations of motion, and the solution technique.

### 1. GENERAL AIRPLANE/RUNWAY MODEL

The general model represents an asymmetrical body with a nose gear and a right and left main landing gear. Each landing gear strut is assumed to have point contact with the profile and it is assumed that each landing gear traverses a different profile. Aerodynamic lift and drag are modeled, and thrust is applied at the aircraft's center of gravity.

The airplane is free to roll, pitch, plunge, and translate horizontally down the runway and each landing gear unsprung mass is free to translate vertically. To these rigid body degrees of freedom, up to 30 flexible modes of vibration are included. This airplane motion is controlled by the landing gear strut forces, lift, drag, thrust, and the resisting parameters of aircraft mass and inertia.

The landing gear struts are nonlinear, single acting oleo pneumatic energy absorbing devices (Figure 2) and are represented in the model as the sum of the three forces; pneumatic, hydraulic, and strut bearing friction forces. The pneumatic force, which is the largest of the three is represented by the equation:

$$F_A = \frac{PV}{\frac{V}{A} - S} \quad (1)$$

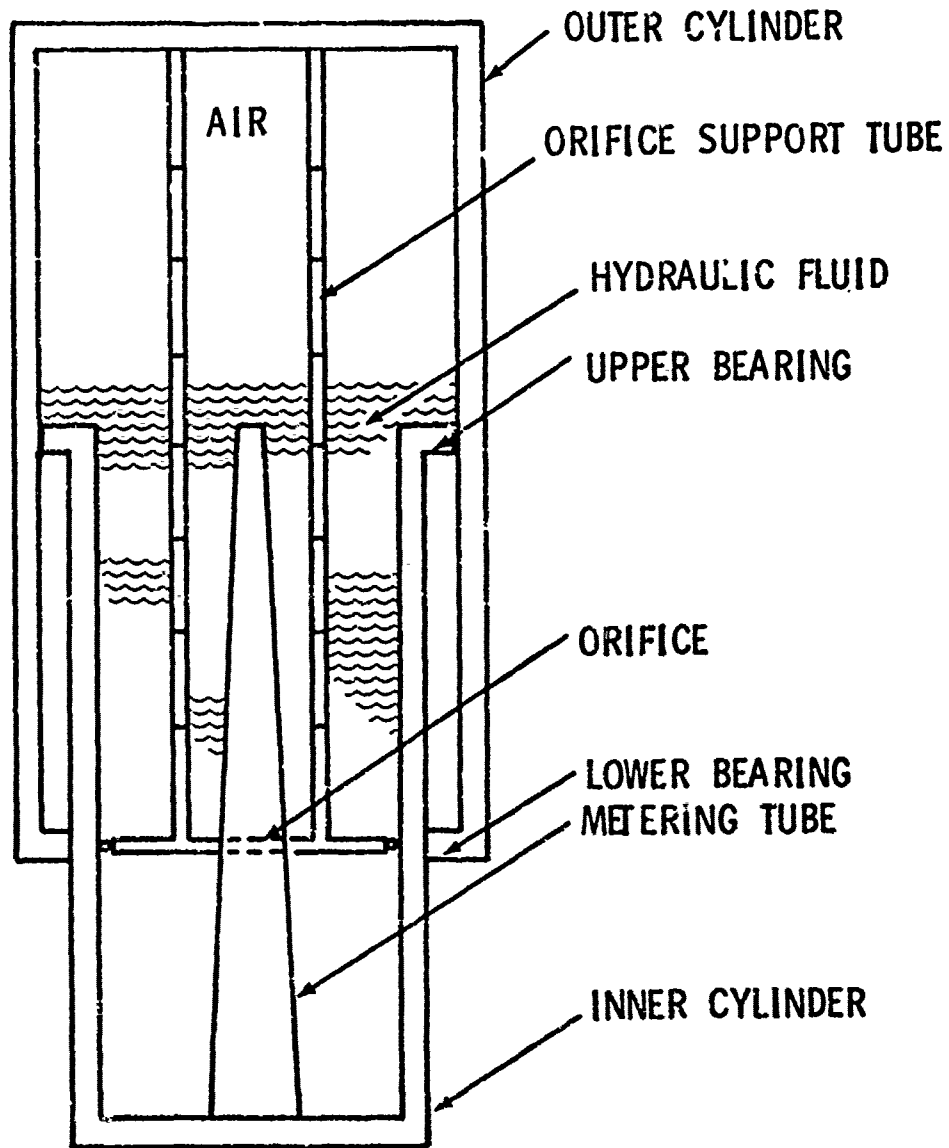


Figure 2. Typical Single Acting Oleo Pneumatic Landing Gear Strut

where:

- P = fully extended strut pressure
- V = fully extended strut volume
- A = pneumatic piston area
- S = strut stroke

The damping force is given by the equation:

$$F_h = \frac{\rho_h A_h^3 \dot{S} |\dot{S}|}{2 (C_d A_o)^2} \quad (2)$$

where:

- $\rho_h$  = density of the hydraulic fluid
- $A_h$  = the hydraulic piston area
- $A_o$  = effective orifice area (constant orifice minus metering pin area)
- $C_d$  = orifice coefficient (use 0.9)
- $\dot{S}$  = strut piston velocity

The third strut force is the strut bearing friction force and is neglected in the model because the force is small for symmetrically loaded struts. (See Reference 2).

The tire force is represented by the linear equation:

$$F_T = k T_D \quad (3)$$

where:

- $T_D$  = tire deflection
- k = linear tire spring constant

The runway elevation data is input into the model in two foot increments. The profile is made continuous by fitting the following

polynomial through the three elevation data points and the slope at the end of the previous profile segment:

$$y(x) = a_1 + a_2x + a_3x^2 + a_4x^3 \quad (4)$$

where:

$a_{1,2,3,4}$  = coefficients derived from the elevation and slope data

This is done for each of the three lines of runway profile data.

## 2. RIGID BODY EQUATIONS OF MOTION

The differential equations of motion for the mathematical model were derived by application of the Lagrange equations (See Appendix A). The general form of these equations is shown below and corresponds to the notation shown in Figure A-1 in Appendix A.

$$\ddot{Z} = (F_{s1*} + F_{s2} + F_{s3} + L - W)/M_{cg} \quad [\text{c.g., vertical acceleration}] \quad (5)$$

$$\ddot{Z}_1 = (F_{t1} - F_{s1} - W_1)/M_1 \quad [\text{unsprung mass vertical acceleration}] \quad (6)$$

$$\ddot{Z}_2 = (F_{t2} - F_{s2} - W_2)/M_2 \quad [\text{unsprung mass vertical acceleration}] \quad (7)$$

$$\ddot{Z}_3 = (F_{t3} - F_{s3} - W_3)/M_3 \quad [\text{unsprung mass vertical acceleration}] \quad (8)$$

$$\ddot{\theta} = (F_{s1}^A + F_{s2}^B + F_{TD}^C - F_{s3}^C)/I_{yy} \quad [\text{pitching acceleration}] \quad (9)$$

$$\ddot{\phi} = (F_{s3} - F_{s2})C/I_{xx} \quad [\text{rolling acceleration}] \quad (10)$$

$$\ddot{X} = (F_T - F_{TD} - F_{AD})/(M_{cg}) \quad [\text{horizontal translation acceleration}] \quad (11)$$

where:

$F_{s1}, F_{s2}, F_{s3}$  = total landing gear strut forces

$F_{t1}, F_{t2}, F_{t3}$  = tire forces

$M_{cg}, W, I_{yy}, I_{xx}$  = aircraft mass, weight, and pitching and roll inertias

\*The subscript 1, 2 and 3 corresponds to the nose, right main and left main landing gears respectively.



- $W_1, W_2, W_3$  = upsprung landing gear weights  
 $A, B, C, \epsilon_1$  = moment arms  
 $L, F_T, F_{TD}, F_{AD}$  = lift, thrust, and tire and aerodynamic drag forces  
 [  $F_T$  and  $F_{AD}$  act through the center of gravity ]

### 3. FLEXIBILITY EQUATIONS OF MOTION

$$M_i \ddot{q}_i = \epsilon_{i1} F_{s1} + \epsilon_{i2} F_{s2} + \epsilon_{i3} F_{s3} - 2\zeta_i \omega_i \dot{q}_i - \omega_i^2 M_i q_i \text{ for the } i\text{th mode}$$

where:

- $M_i$  = the generalized mass  
 $\epsilon_{i1}, \epsilon_{i2}, \epsilon_{i3}$  = modal deflections at gear location 1, 2 and 3  
 $\omega_i$  = modal frequency  
 $\zeta$  = damping factor  
 $q_i = \dot{q}_i, \ddot{q}_i$  = generalized coordinates and their time derivatives.

The sign convention is as follows:

- $Z$  = Vertical Displacement + up  
 $\theta$  = Pitch + nose down  
 $\phi$  = Roll + roll right  
 $q$  = Deflection Due to Bending + up  
 $X$  = Horizontal Translation + forward

### 4. SOLUTION TECHNIQUE

The technique used for solving the coupled nonlinear differential equations of motion that describe the simulated aircraft is a three-term Taylor series. For example, the equation:

$$\ddot{x} = -c\dot{x} - kx \quad (12)$$

The three term Taylor series representations can be written as

$$x_{(I+1)} = x_{(I)} + \dot{x}_{(I)} (\Delta t) + \ddot{x}_{(I)} \frac{(\Delta t)^2}{2} \quad (13)$$

where:  $I = 1 \rightarrow N$

The values for  $\ddot{x}$ ,  $\dot{x}$  and  $x$  from the previous step are substituted into Equation 13 and a new value for  $x$  is obtained. Differentiating Equation 13 we obtain for the velocity  $\dot{x}$ , the expression:

$$\dot{x}_{(I+1)} = \dot{x}_{(I)} + \ddot{x}_{(I)} (\Delta t) \quad (14)$$

The values for  $\dot{x}$  and  $\ddot{x}$  are then substituted into Equation 14 and a new value of  $\dot{x}$  is found. This entire process is repeated with the new values of  $x$  and  $\dot{x}$  to obtain the next point in the solution.

SECTION III  
COMPUTER PROGRAM

The computer program, TAX2, which computes the dynamic response of a flexible aircraft to an asymmetrical runway profile, consists of one basic program and several subroutines. A complete listing of the program is contained in Appendix B. Table 1 contains a description of the aircraft input data and Figure 3 shows the source deck setup for use on the CDC 6600 computer at Wright-Patterson AFB, Ohio.

1. OUTPUT FORMAT

The results of the calculations are presented as both a printed output and a time history plot. The printed output lists the value of fifteen parameters each 0.01 second. A sample of this listed output is shown in Table 2. The fifteen parameters listed in the heading are:

XMAINL	-	Left Main landing gear strut deflection (inches)
XMAINR	-	Right Main landing gear strut deflection (inches)
XNOSE	-	Nose gear strut deflection (inches)
ZPML	-	Left Main landing gear runway elevation (inches)
ZPMR	-	Right Main landing gear runway elevation (inches)
ZPN	-	Nose landing gear runway elevation (inches)
BETADD	-	Rolling acceleration ( $\ddot{\phi}$ ) (rad/sec <sup>2</sup> )
THETADD	-	Pitching acceleration ( $\ddot{\theta}$ ) (rad/sec <sup>2</sup> )
BETA	-	Roll angle ( $\phi$ ) (rad)
THETA	-	Pitch angle ( $\theta$ ) (rad)
SPEED	-	Aircraft velocity (ft/sec)
DISTANCE	-	Distance traveled down the runway (feet)
TIME	-	Real time (seconds)
CGACC	-	Center of Gravity Vertical Acceleration (g's)
PSA	-	Pilot's Station Vertical Acceleration (g's)

Figure 4 shows a photographic reduction of a typical Calcomp-plotted time history. This figure depicts a Boeing 727-100 taxiing at 50 fps over a 1-cos bump at a 45° angle of approach. The plotted output includes titles showing the airplane simulated, its gross weight,

TABLE 1  
DESCRIPTION OF INPUT AIRCRAFT DATA  
Section 1 (cards 1-5) - General Airplane Data

Card Column	Format	Variable Name	Data for McDonnell-Douglas C-9A	Definition
<u>Card 1</u>				
1-80	8A10	PLANE	McDonnell-Douglas C-9A	Airplane Being Simulated and Gross Weight
<u>Card 2</u>				
1-10	F10.1	W	108000.	Vehicle Weight (lbs)
11-20	F10.1	A	51.6	Distance Main Gear to CG (in)
21-30	F10.1	B	589.4	Distance Nose Gear to CG (in)
31-40	F10.1	MMI	20800000.	Pitch Moment of Inertia (lb in sec <sup>2</sup> )
41-52	F12.0	WS	96.	Wing Station of Main Gear (in)
53-64	F12.0	MMIR	8000000.	Roll Moment of Inertia (lb in sec <sup>2</sup> )
<u>Card 3</u>				
1-10	F10.2	PSARM	607.0	Distance of Pilot Station to CG (in)
11-20	F10.2	TAILRM	318.5	Distance of Tail Station to CG (in)
<u>Card 4</u>				
1-10	F10.2	SPEED	50.	Initial Velocity of Airplane (ft/sec)
11-20	F10.2	THRUST	29000.	Total Airplane Thrust (lbs)
21-30	F10.2	TAKEOFF	285.5	Airplane Rotation Speed (ft/sec)

TABLE 1 (Continued)

Card Column	Format	Variable Name	Data for McDonnell-Douglas C-9A	Definition
<u>Card 5</u>				
1-10	F10.4	CL	1.1	Lift Coefficient
11-20	F10.4	AREA	1000.7	Wing Area (ft <sup>2</sup> )
21-30	F10.4	CD	.1	Drag Coefficient
<u>Section 2 (cards 6-11) - Main and Nose Gear</u>				
<u>Card 6</u>				
1-10	F10.2	WM	957.16	Unsprung Weight of Each Main Gear (lbs)
11-20	F10.2	WN	153.43	Unsprung Weight of Nose Gear (lbs)
21-30	F10.2	SXM	2.	Number of Main Gear Struts
31-40	F10.2	SXN	1.	Number of Nose Gear Struts
<u>Card 7</u>				
1-10	F10.5	AHN	6.745	Hydraulic Piston Area Nose (in <sup>2</sup> )
11-20	F10.5	AAN	8.2958	Pneumatic Piston Area Nose (in <sup>2</sup> )
21-30	F10.5	AHM	16.5	Hydraulic Piston Area Main (in <sup>2</sup> )
31-40	F10.5	AAM	21.648	Pneumatic Piston Area Main (in <sup>2</sup> )
<u>Card 8</u>				
1-10	F10.5	PAOH	120.	Nose Strut Preload Pressure (lbs/in <sup>2</sup> )
11-20	F10.5	PACM	220.	Main Strut Preload Pressure (lbs/in <sup>2</sup> )

TABLE 1 (Continued)

Card Column	Format	Variable Name	Data for McDonnell-Douglas C-9A	Definition
21-30	F10.5	VON	126.2	Fully Extended Nose Strut Air Volume (in <sup>3</sup> )
31-40	F10.5	VOM	366.0	Fully Extended Main Strut Air Volume (in <sup>3</sup> )
41-50	F10.5	OAM	.543	Orifice Area Main (in <sup>2</sup> )
51-60	F10.5	OAN	.442	Orifice Area Nose (in <sup>2</sup> )
<u>Card 9</u>				
1-10	F10.3	SLM	85.5	Distance from Axle to CG Waterline Main Gear Strut Unloaded (in)
11-20	F10.3	SLN	87.3	Distance from Axle to CG Waterline Nose Gear Strut Unloaded (in)
<u>Card 10</u>				
1-10	F10.1	TSM	23428.6	Main Tire Spring Constant Per Strut (lbs/in)
11-20	F10.1	TSN	8632.5	Nose Tire Spring Constant Per Strut (lbs/in)
<u>Card 11</u>				
1-10	F10.5	DX	.001	Integration Step Size
<u>Card 12</u>				
1-5	I5	IFPLOT	0	0-Plot; 1-No Plot
6-10	I5	IFLIST	0	0-List; 1-No List
<u>Section 3 (cards 13-16) - Metering Pin Description</u>				
<u>Card 13</u>				
1-5	I5	NSCN	5	Number of Slope Changes Nose Gear

TABLE 1 (Continued)

Card Column	Format	Variable Name	Data for McDonnell-Douglas C-9A	Definition
<u>* Card 14A, 14B,....</u>				
1-10	F10.3	STROKN (1)	*	Stroke Corresponding to Metering Pin Diameter, Nose Gear
11-20	F10.3	PINDN (1)	*	Metering Pin Diameter, Nose Gear (in)
<u>Card 15</u>				
1-5	I5	NSCM	*	Number of Slope Changes Main Gear
<u>* Card 16A, 16B,....</u>				
1-10	F10.3	STROKM (1)	*	Stroke Corresponding to Metering Pin Diameter, Nose Gear
11-20	F10.3	PINDM (1)	*	Metering Pin Diameter, Main Gear (in)
<u>Section 4 (cards 17-19) - Flexibility Data</u>				
<u>Card 17</u>				
1-5	I5	NFM	7	Number of Symmetrical Flexible Modes
6-10	I5	NAFM	7	Number of Asymmetrical Modes
<u>** Card 18A, 18B,....</u>				
1-10	F10.3	SIMAIN (1)	**	Mode Shape Deflection Main Gear
11-20	F10.3	SINOSE (1)	**	Mode Shape Deflection Nose Gear
21-30	F10.3	SICG (1)	**	Mode Shape Deflection CG
31-40	F10.3	SITAIL (1)	**	Mode Shape Deflection Tail Station

TABLE 1 (Continued)

Card Column	Format	Variable Name	Data for McDonnell-Douglas C-9A	Definition
41-50	F10.3	SIPS	**	Mode Shape Deflection Pilot Station
<b>** Card 19A, 19B,....</b>				
1-15	F15.2	GM (I)	**	Generalized Mass (lbs sec <sup>2</sup> /in)
16-25	F10.3	OMEGA (I)	**	Modal Frequency (rad/sec)
<b>** Card 20A, 20B,....</b>				
1-10	F10.3	SILEFT (I)	**	Deflection for Left Main Gear
11-20	F10.3	SIRIGHT (I)	**	Deflection for Right Main Gear
<b>** Card 21A, 21AB,....</b>				
1-15	F15.3	GMA (I)	**	Asymmetrical Generalized Mass (lbs sec <sup>2</sup> /in)
16-25	F10.4	OMEGAA (I)	**	Asymmetrical Modal Frequency (rad/sec)

\* One card is required for each stroke-metering pin combination read into the program.

\*\* One card is required for each flexible mode.

Note: A summary of all the data used in this study is shown in Appendix C.



TABLE 1 (Concluded)

Runway Profile Magnetic Tape

The runway profile is read into the program from a magnetic tape or permanent file. The format for this is shown below:

Column	Format	Variable Name	Definition
<u>Read 1</u>			
1-80	8A10	SITE**	Runway Profile and Direction
<u>Read 2</u>			
1-6	I6	NPTSS**	Number of Runway Elevation Points
<u>* Read 3, 4, ..., N+2</u>			
1-70	10F7.3	ELEVL**	Runway Profile Data
		ELEV	
		ELEVR	

\* One read required for every ten runway profile elevation points.

\*\* The process is repeated for each of the three profiles.

Note: All of the runway profile data used in this study is listed in Appendix D.

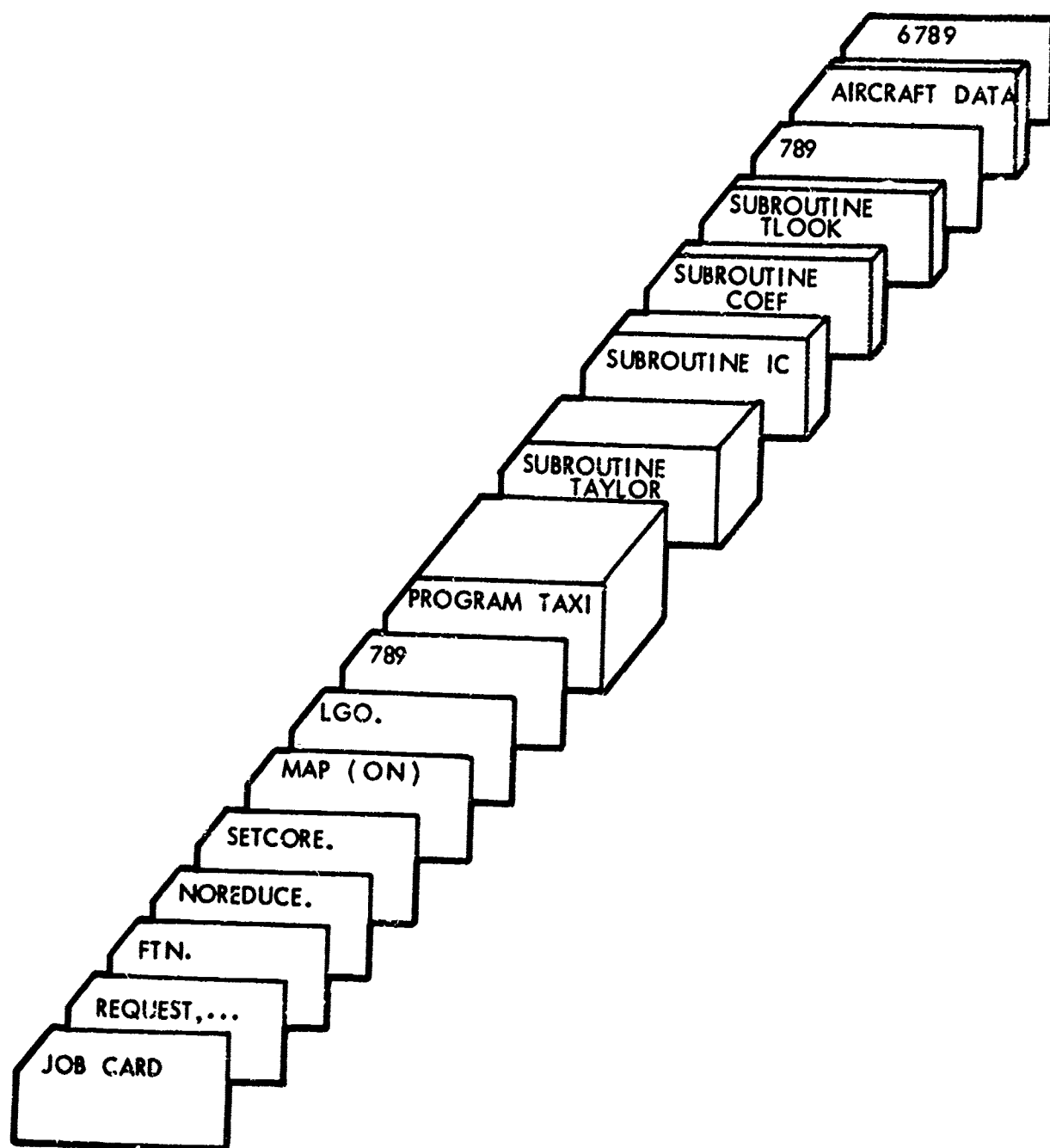


Figure 3. Source Deck Setup

# BEST AVAILABLE COPY

THESE ARE THE RESULTS OF THE COMPUTATION OF THE SECOND ORDER CORRECTION TO THE FIRST ORDER SOLUTION OF THE PROBLEM OF THE MOTION OF A PARTICLE IN A MEDIUM WITH A SPHERICALLY SYMMETRIC INDEX OF REFRACTION. THE RESULTS ARE GIVEN IN TABLES 1 AND 2.

THE COMPUTATION WAS PERFORMED USING A DIGITAL COMPUTER. THE PROGRAM WAS WRITTEN IN FORTRAN. THE RESULTS ARE GIVEN IN TABLES 1 AND 2.

THE RESULTS ARE GIVEN IN TABLES 1 AND 2.

THE RESULTS ARE GIVEN IN TABLES 1 AND 2.

THE RESULTS ARE GIVEN IN TABLES 1 AND 2.

THE RESULTS ARE GIVEN IN TABLES 1 AND 2.

THE RESULTS ARE GIVEN IN TABLES 1 AND 2.

THE RESULTS ARE GIVEN IN TABLES 1 AND 2.

THE RESULTS ARE GIVEN IN TABLES 1 AND 2.

THE RESULTS ARE GIVEN IN TABLES 1 AND 2.

THE RESULTS ARE GIVEN IN TABLES 1 AND 2.

THE RESULTS ARE GIVEN IN TABLES 1 AND 2.

THE RESULTS ARE GIVEN IN TABLES 1 AND 2.

THE RESULTS ARE GIVEN IN TABLES 1 AND 2.

THE RESULTS ARE GIVEN IN TABLES 1 AND 2.

THE RESULTS ARE GIVEN IN TABLES 1 AND 2.

TABLE 2  
TYPICAL COMPUTER OUTPUT LISTING

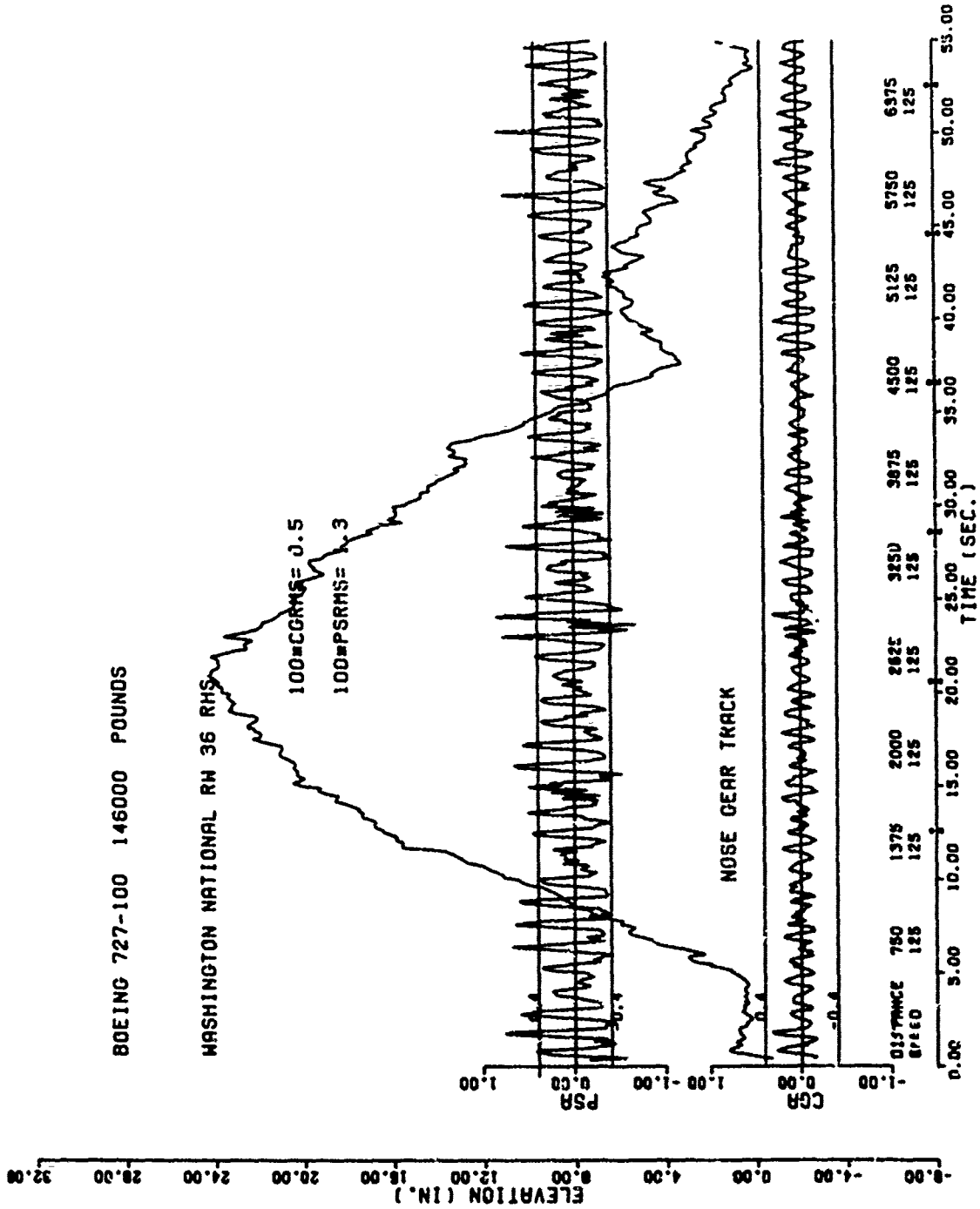


Figure 4. Typical Calcomp Plotted Output

the runway number and its location. The abscissa is the time axis annotated every second. At every time annotation the current value of aircraft speed, in feet per second, and the current aircraft position on the runway, in feet, are printed out. Runway markers (1,000-foot markers) are also plotted on the time scale to aid in aircraft positioning. The plot titled "Nose Gear Track" is a time history of the runway profile as it is encountered by the aircraft's nose gear. The actual runway profile is preceded by 100 feet of smooth surface to allow any starting transients to damp out prior to encountering the actual profile. There are two aircraft acceleration time histories that are of particular interest. One is the vertical acceleration at the pilot's station (PSA), the other is the vertical acceleration at the aircraft's center of gravity (CGA). Each time history is banded by the human tolerance criterion of  $\pm 0.4$  g. In order to minimize the amount of computer central memory required to store the acceleration time histories, the higher frequency components were effectively filtered out by limiting the sampling interval. All of the acceleration peaks, however, are shown on the plot. It should be noted that the pilot station acceleration time history is not always within the band of accepted human tolerance criteria. Thus, the plot is very useful in that it provides a graphical record of the level of acceleration, and it shows which bumps in the runway profile caused the high acceleration response.

#### SECTION IV DISCUSSION OF SIMULATIONS

Table 3 contains a summary of the simulations made in this study. Three different airplanes were simulated: the Boeing 727-100, the McDonnell Douglas C-9A, and an AMST configuration. Each airplane was simulated traversing two profiles: Washington National Runway 36, and a 1-cos dip. Simulations were made using mathematical models with and without a roll degree of freedom, i.e. one or three profiles, and with and without flexible wings so that comparisons of the responses could be made.

Figures 5 and 6 show the plotted results of a Boeing 727-100 traversing the Washington National runway profile without a roll degree of freedom and with a roll degree of freedom respectively. Both runs were made at a constant speed of 125 feet per second, because this speed produced higher levels of vertical acceleration for this airplane. Comparison of these two figures shows a significant increase in the vertical acceleration at the pilot's station (P.S.) while the aircraft is at different locations on the runway. For example, at T=46 sec. P.S. acceleration levels more than doubled when three lines of profile were used. This is attributed to the fact that the profiles seen by the main landing gear were rougher in the latter case. Figure 7 shows the Power Spectral Density (PSD) levels of each line of survey for the Washington National runway. A PSD is a measure of the relative roughness of a runway versus frequency. It can be seen that the PSD level is different for each line of survey which accounts for the change in the aircraft's dynamic response. Figures 8 and 9 show the 727-100 traversing a 1-cos dip headon and at a 45° angle respectively. In this case the speed was 50 fps which "tunes" the natural pitching frequency (1 cps) of the 727-100 to this 1-cos dip. Hitting the 1-cos dip at an angle caused an increase in the peak P.S. and C.G. acceleration levels.

It was necessary to try to simulate different aircraft with the computer program in an effort to check the program's versatility.

TABLE 3  
SUMMARY OF SIMULATIONS

Run #	Airplane	Profile	Speed	Remarks
1	727-100	Washington National (C)	125 fps	No Roll DOF <sup>*</sup> , Rigid Wings
2	727-100	Washington National (L,C,R)	125 fps	With Roll DOF, Rigid Wings
3	727-100	(1-cos) (C)	50 fps	No Roll DOF, Rigid Wings
4	727-100	(1-cos) (L,C,R)	50 fps	With Roll DOF, Rigid Wings
5	C-9A	(1-cos) (L,C,R)	50 fps	With Roll DOF, Rigid Wings
6	AMST	(1-cos) (L,C,R)	50 fps	With Roll DOF, Rigid Wings
7	727-100	Washington National (L,C,R)	Takeoff	With Roll DOF, Rigid Wings
8	AMST	Washington National (L,C,R)	Takeoff	With Roll DOF, Rigid Wings
9	C-9A	Washington National (L,C,R)	Takeoff	With Roll DOF, Rigid Wings
10	C-9A	(1-cos) (L,C,R)	50 fps	With Roll DOF, Flexible Wings
11	C-9A	Washington National (L,C,R)	Takeoff	With Roll DOF, Flexible Wings

---

\* Degree of Freedom

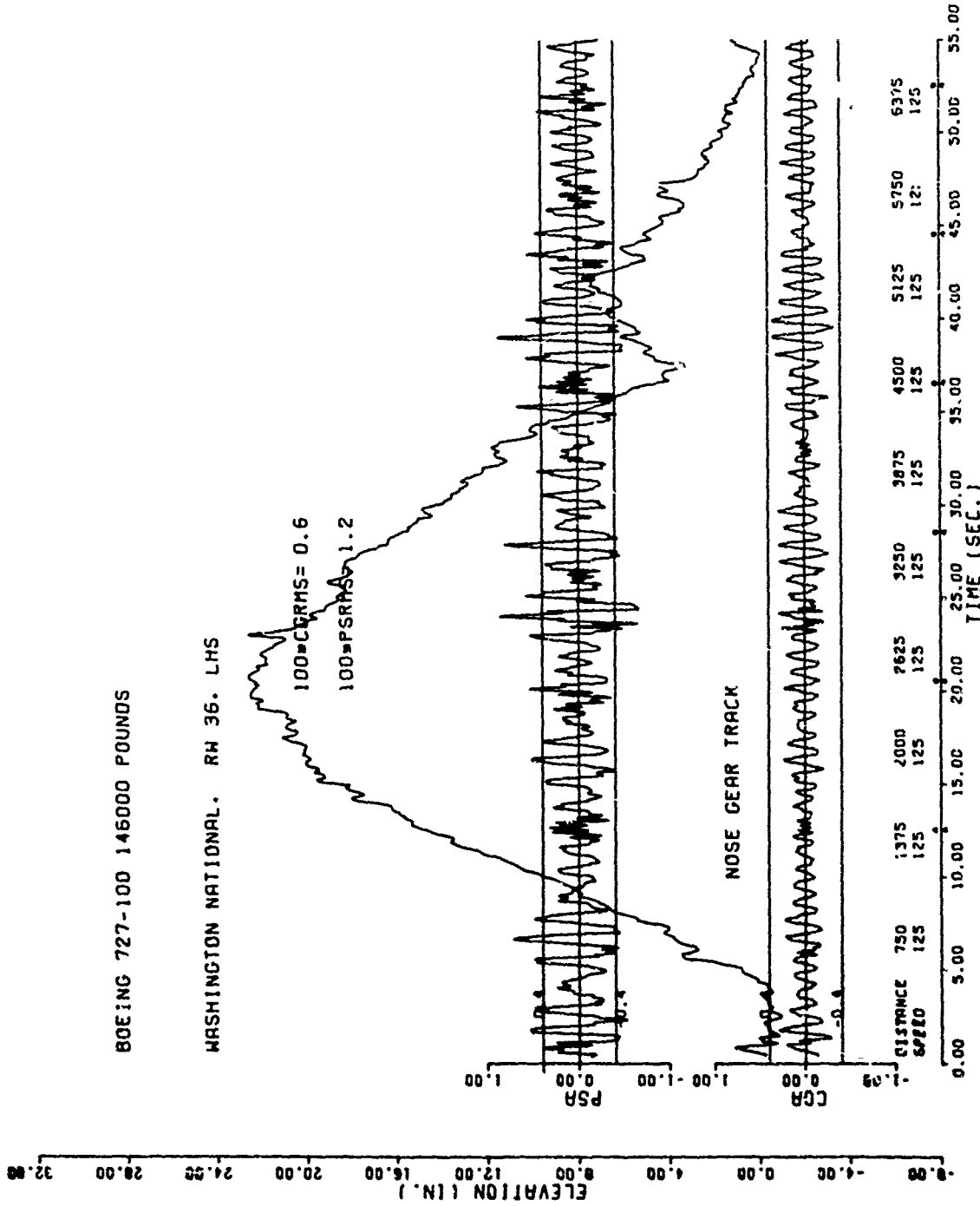


Figure 5. Boeing 727-100 Constant Speed Taxi Simulation over the Washington National Profile Without a Roll Degree of Freedom



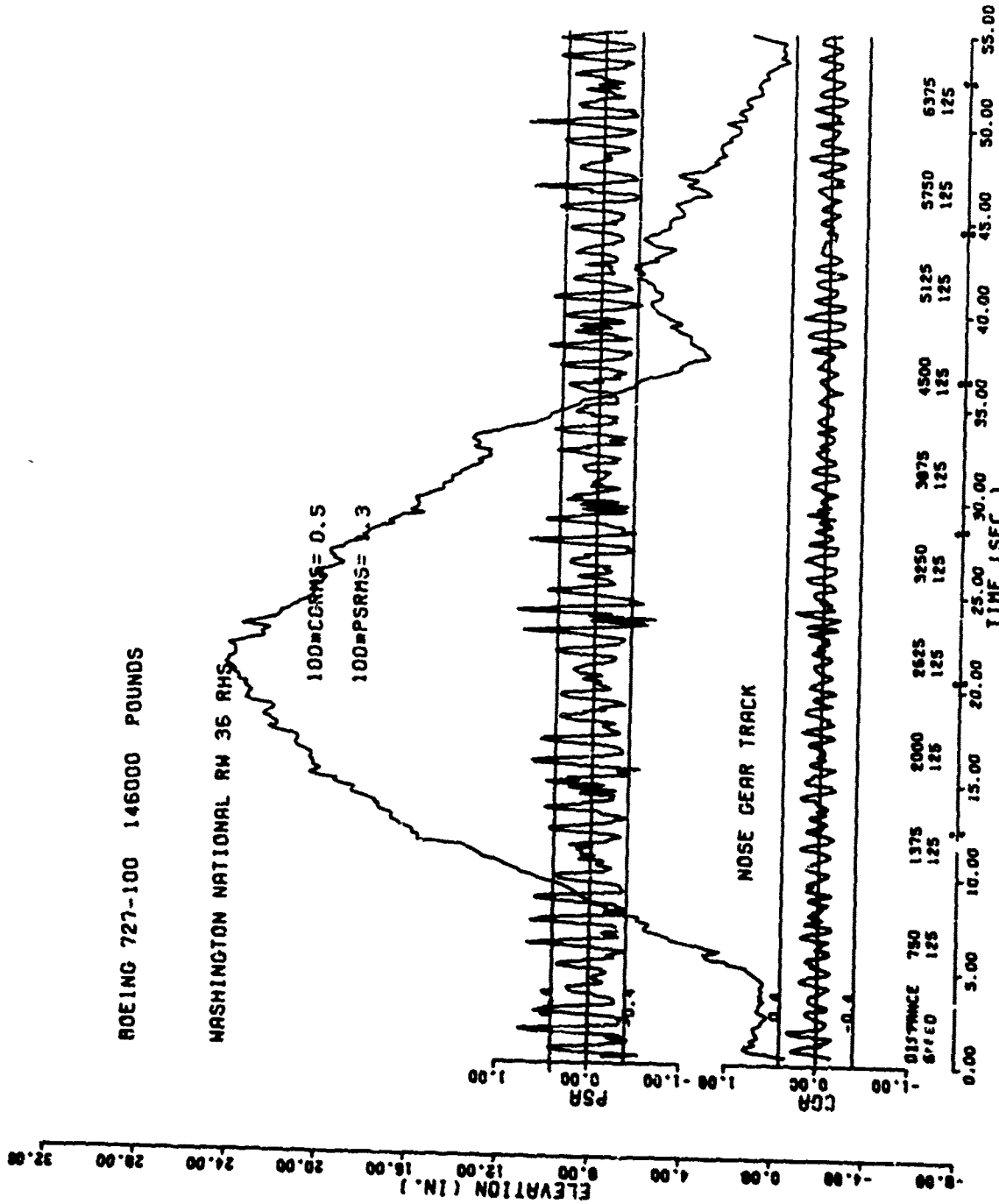


Figure 6. Boeing 727-100 Constant Speed Taxi Simulation over the Washington National Profile with a Roll Degree of Freedom

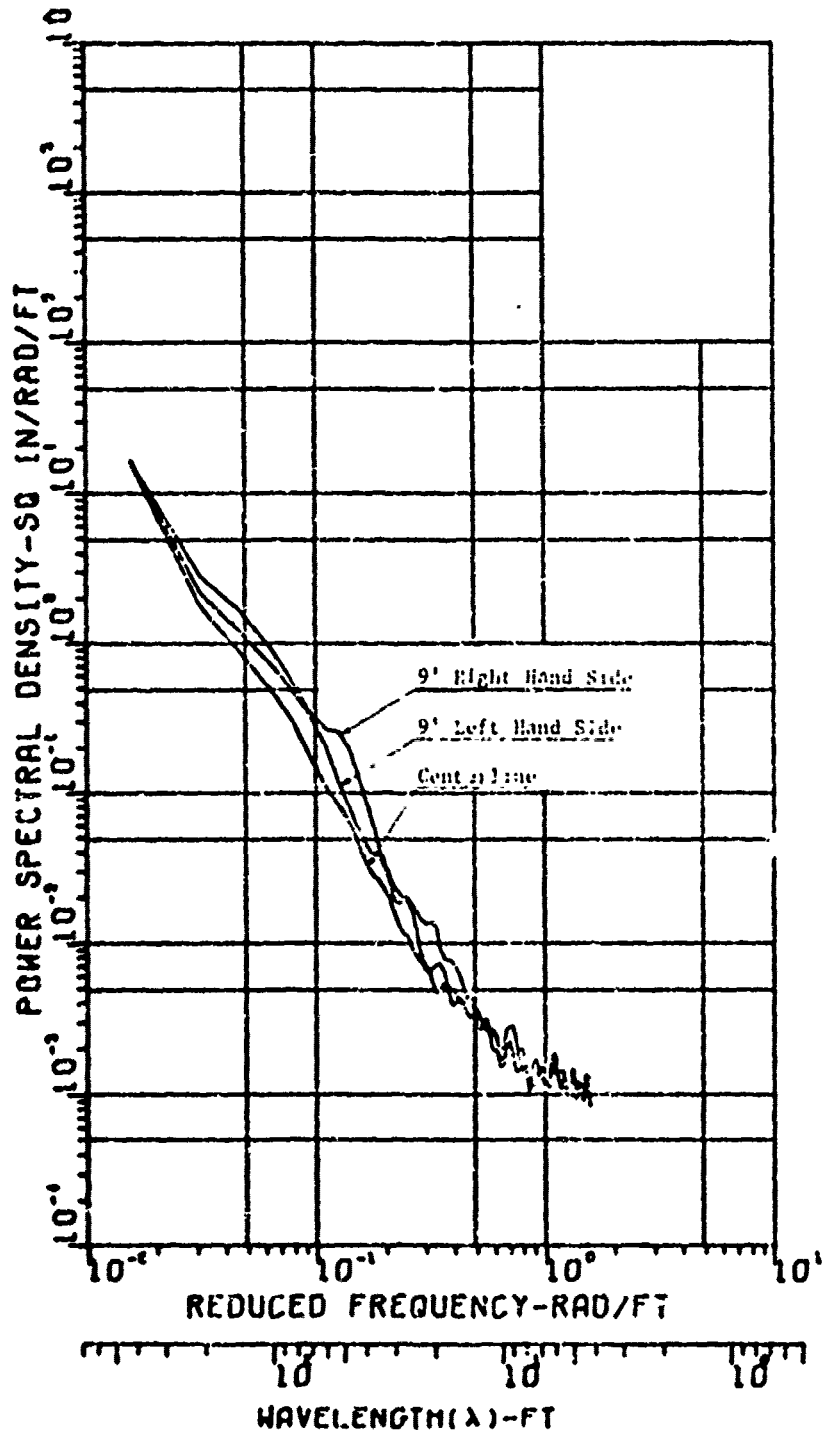


Figure 7. PSD of Washington National Airport Runway 36

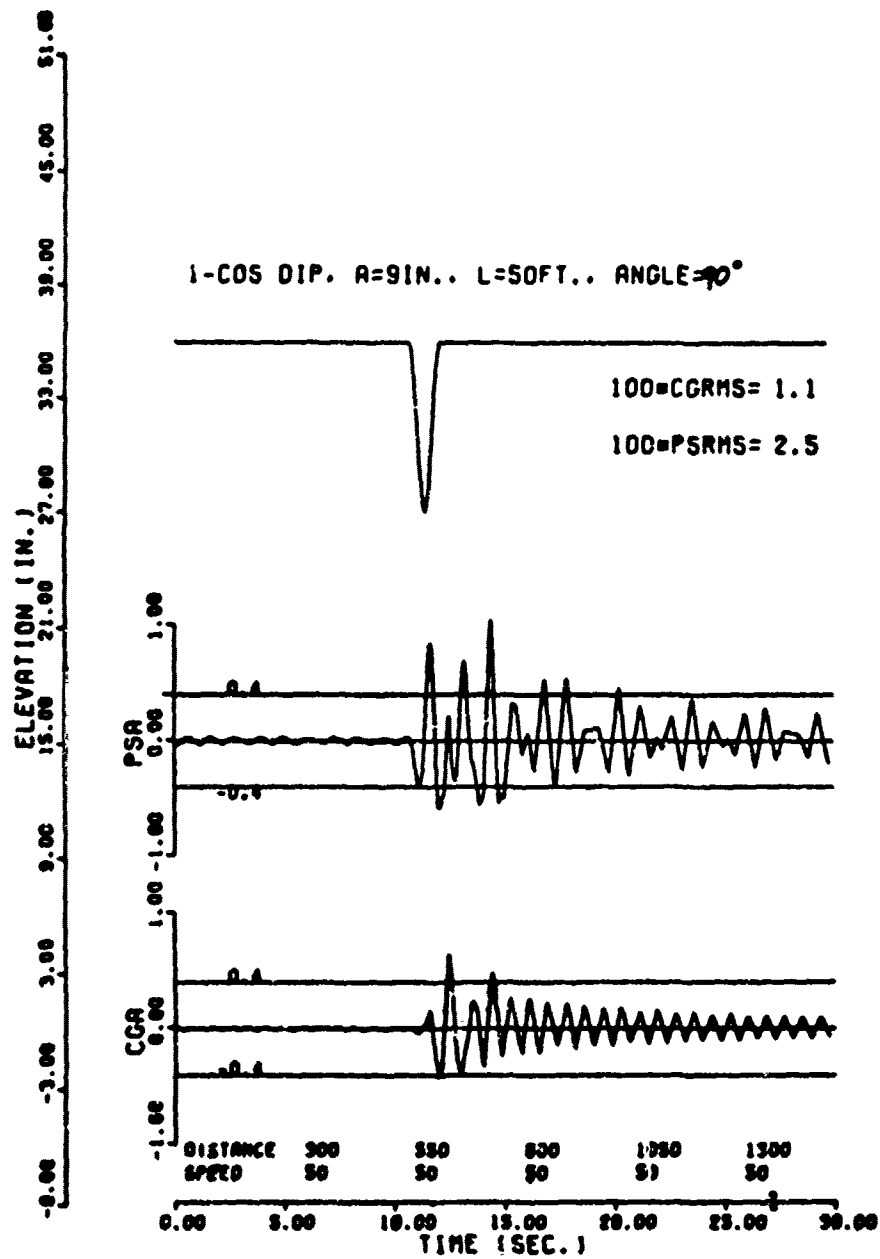


Figure 8. Boeing 727-100 Traversing a (1-cos) dip head-on.

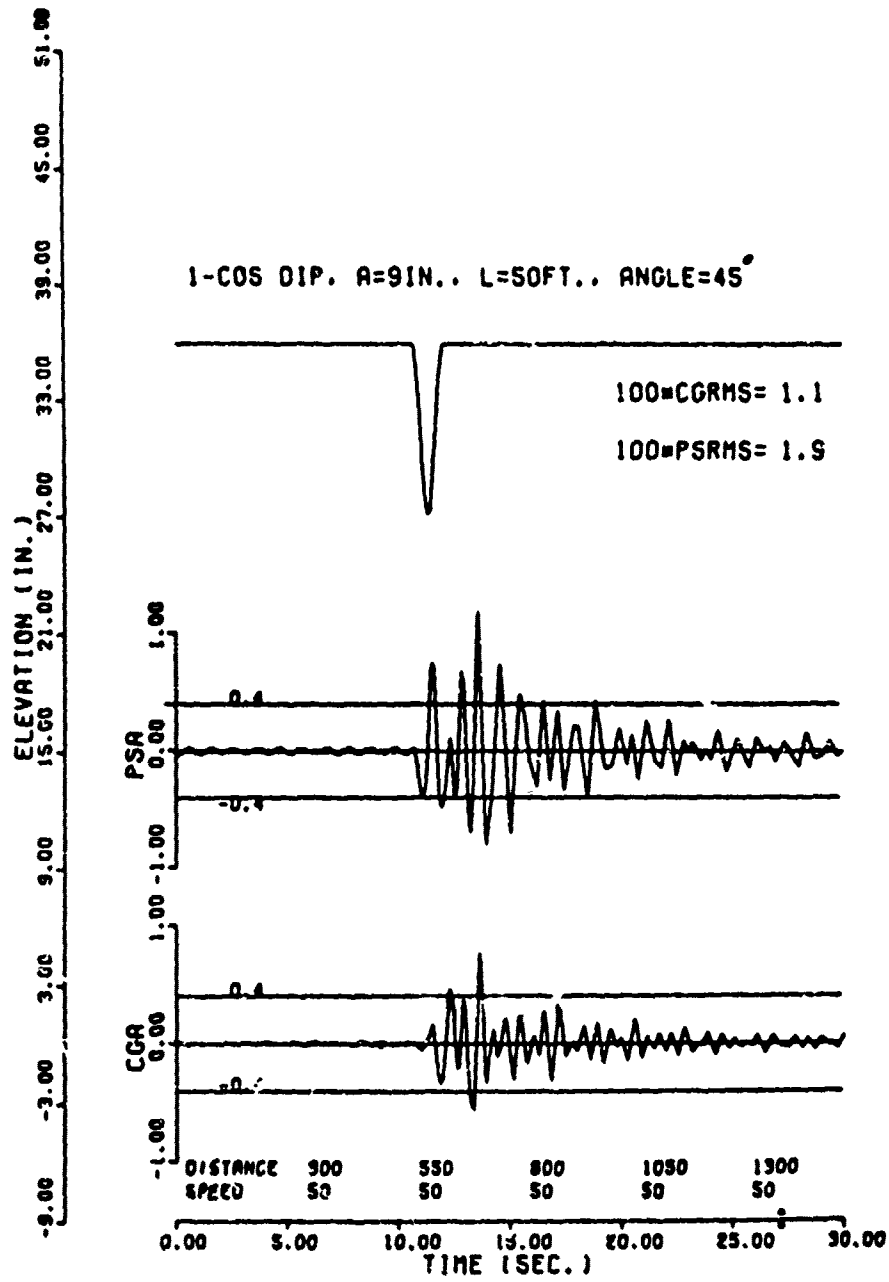


Figure 9. Boeing 727-100 Traversing a (1-cos) dip at a 45° angle

Figures 10 and 11 show the plotted results of the C-9A and AMST respectively hitting the 1-cos dip at a 45° angle at a constant speed of 50 fps. While the C-9A had a relatively high response, the AMST, which is designed to operate off of rough fields, "absorbed" the dip to a large degree. This indicates that the computer program is calculating relative responses which are at least intuitively correct.

Up to this point only constant speed simulations have been discussed. Figures 12, 13 and 14 show the plotted results of the Boeing 727-100, AMST and the C-9A respectively taking off from the Washington National runway profile. Takeoff simulations are made by starting at a near zero forward velocity and accelerating at a constant thrust until rotation speed is reached, then the simulation is terminated. Again it can be seen that the AMST (which is designed for rough field operation) had a very low dynamic response, even though this runway is relatively rough. Figure 15 shows the plotted PSD's of Washington National Runway 36 and of two typically smooth runways, one at Portland Oregon and one at Dulles International. The Washington National Runway is significantly rougher.

Experimental data was available for comparison with the 727-100 takeoff simulation. Figure 16 shows the actual time history plots of vertical acceleration measured on a 727-100 taking off at 120,000 pounds gross weight from Washington National Runway 36 on December 11, 1972. Some parameters of the test aircraft were unknown such as strut and tire pressures and actual inertias. So exact simulation was not possible. However, Table 4 shows that comparison of several peak values of vertical accelerations at the P.S. were within 15 percent. The comparisons of C.G. vertical accelerations were not as good. In the simulation the acceleration levels were lower. It appears that main gear strut pressures on the actual airplane were lower than that simulated. This difference would cause the higher response in the plunge mode.

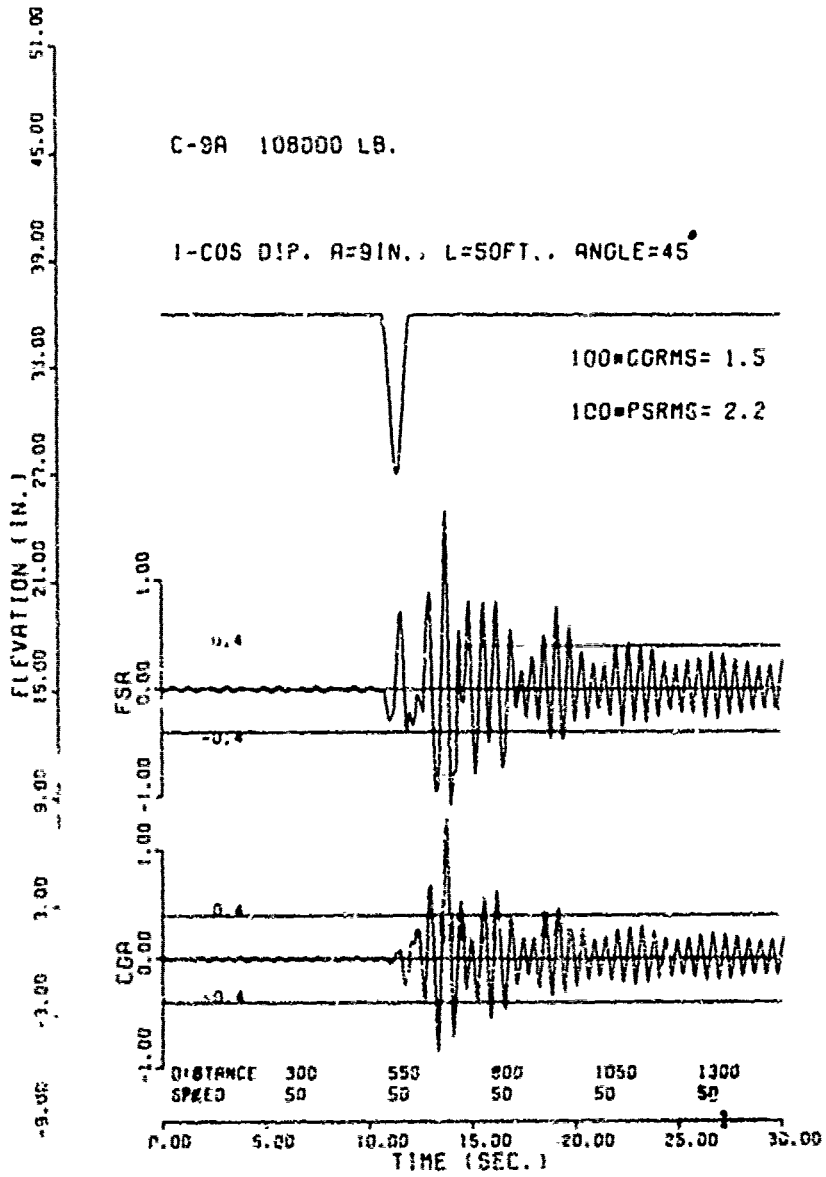


Figure 10. C-9A Traversing a (1-cos) dip at a 45° angle

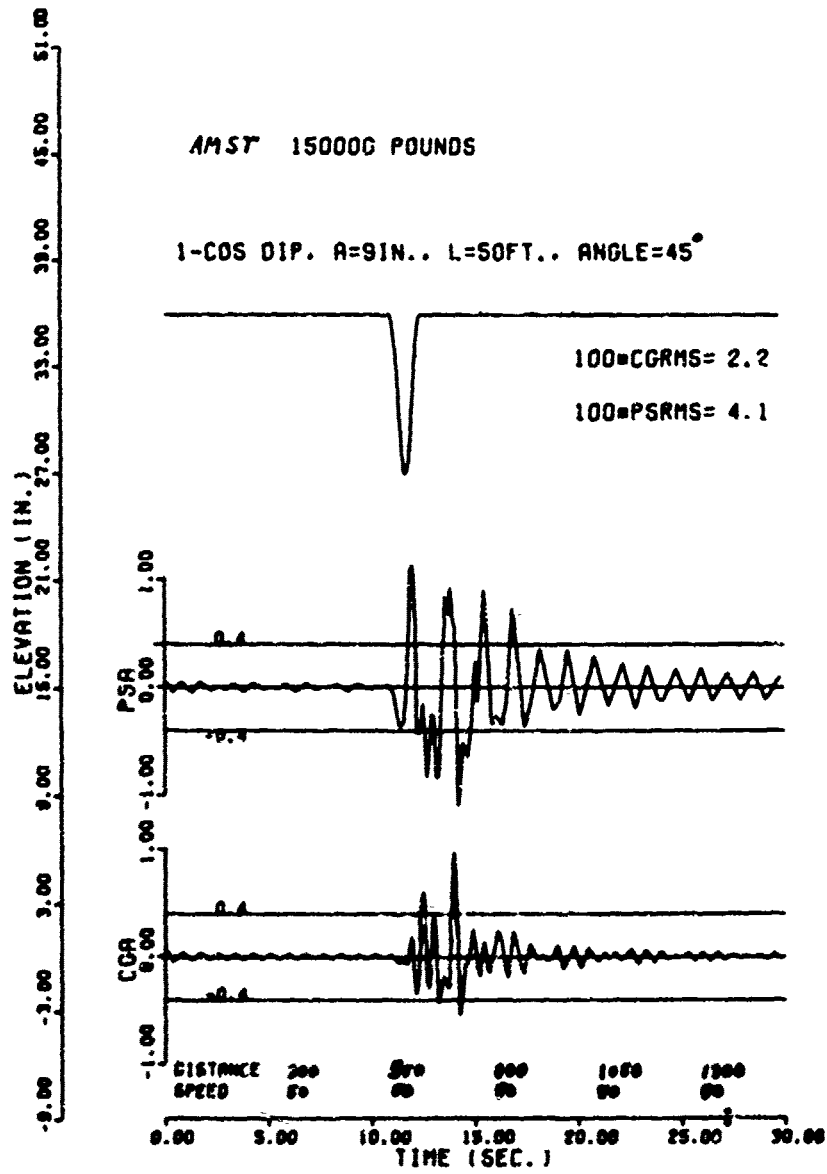


Figure 11. AMST Traversing a (1-cos) dip at a 45° angle

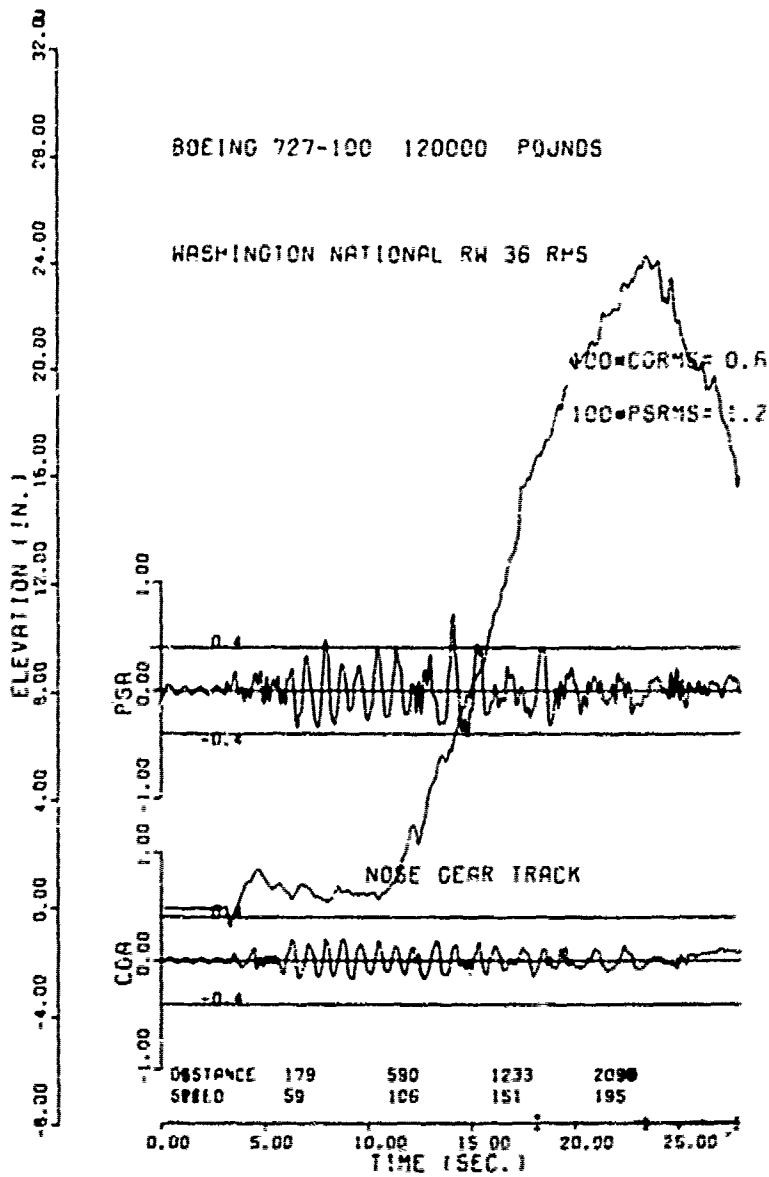


Figure 12. Boeing 727-100 Taking Off from Washington National Airport With the Roll Degree of Freedom Included



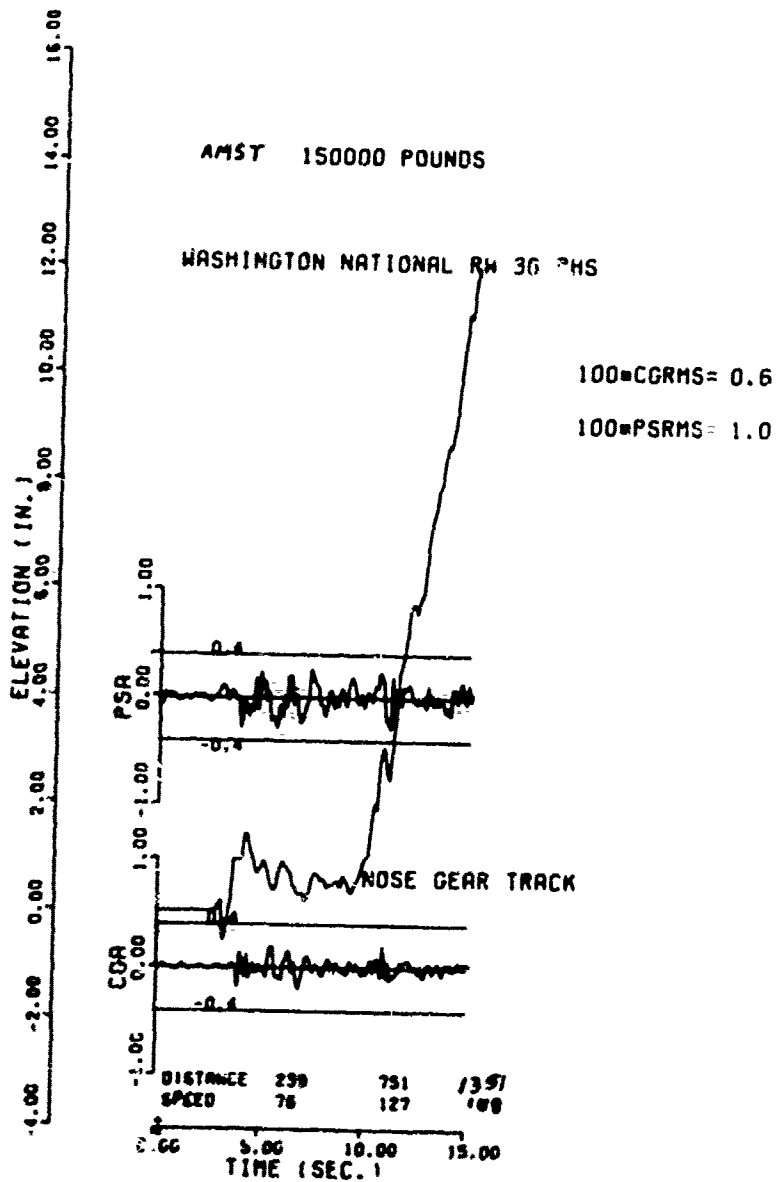


Figure 13. AMST Taking Off from Washington National Airport With the Roll Degree of Freedom Included

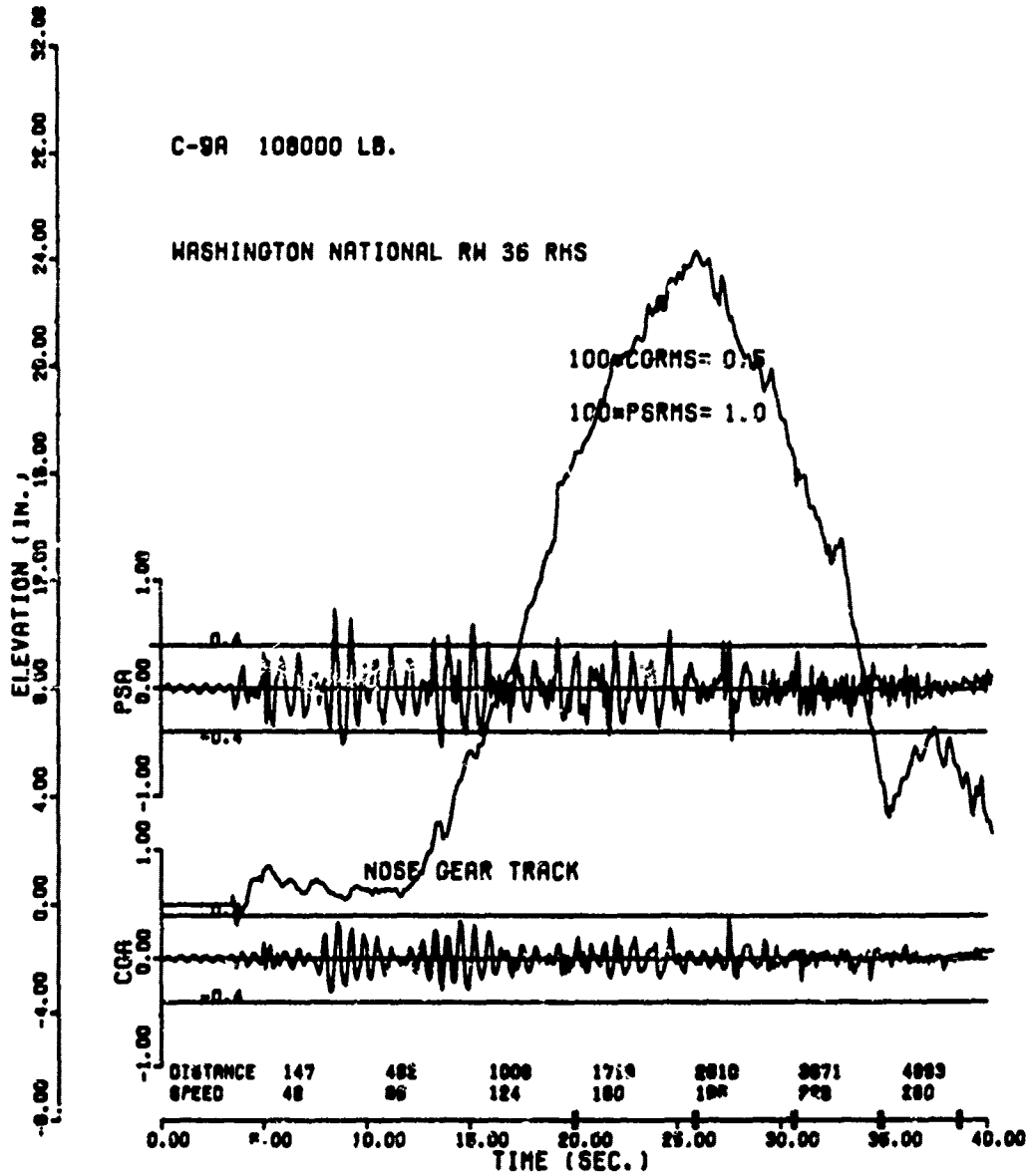


Figure 14. C-9A Taking Off from Washington National Airport With the Roll Degree of Freedom Included

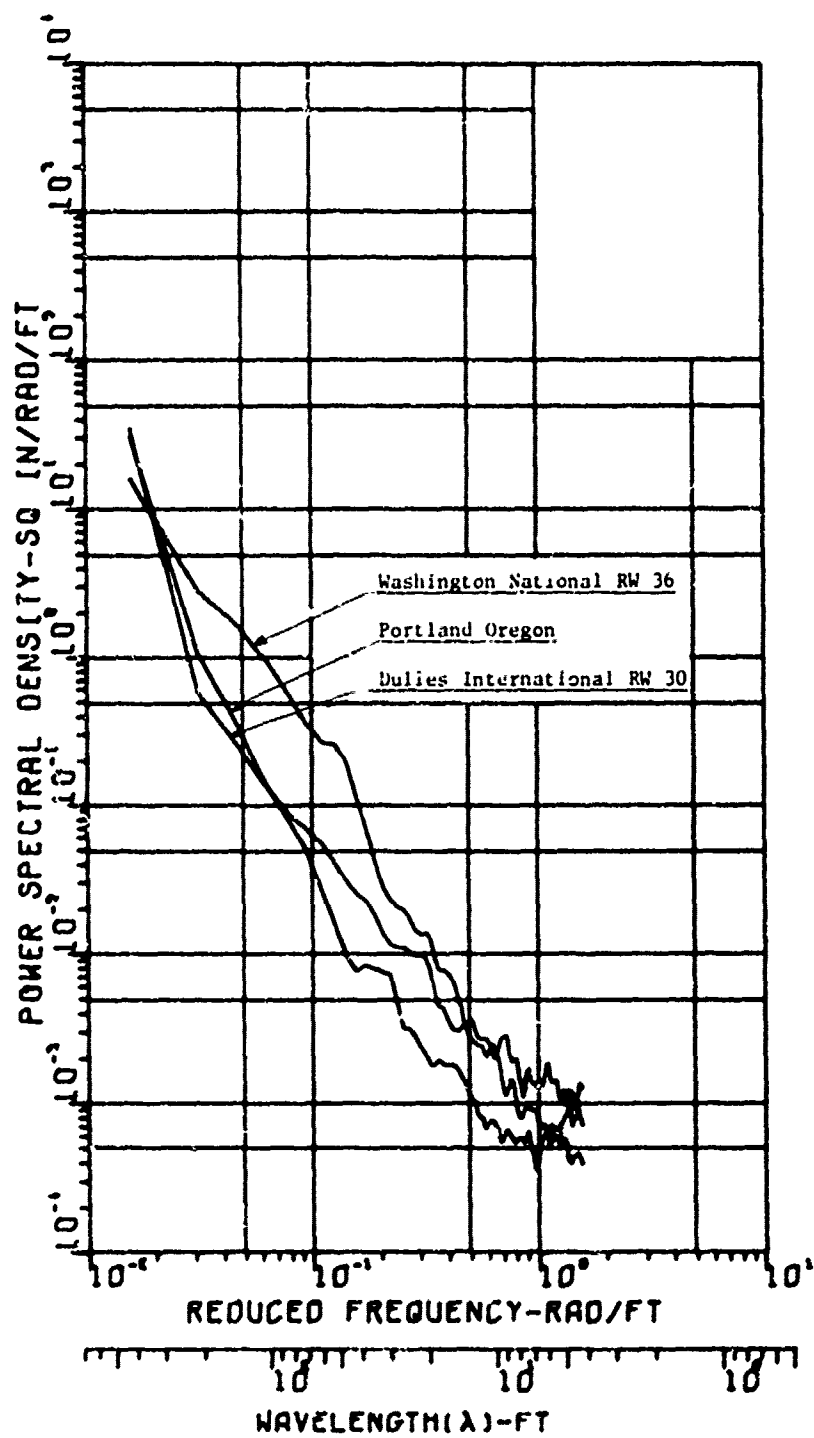


Figure 15. PSD of Washington National Runway 36 and two Typically Smooth Runways

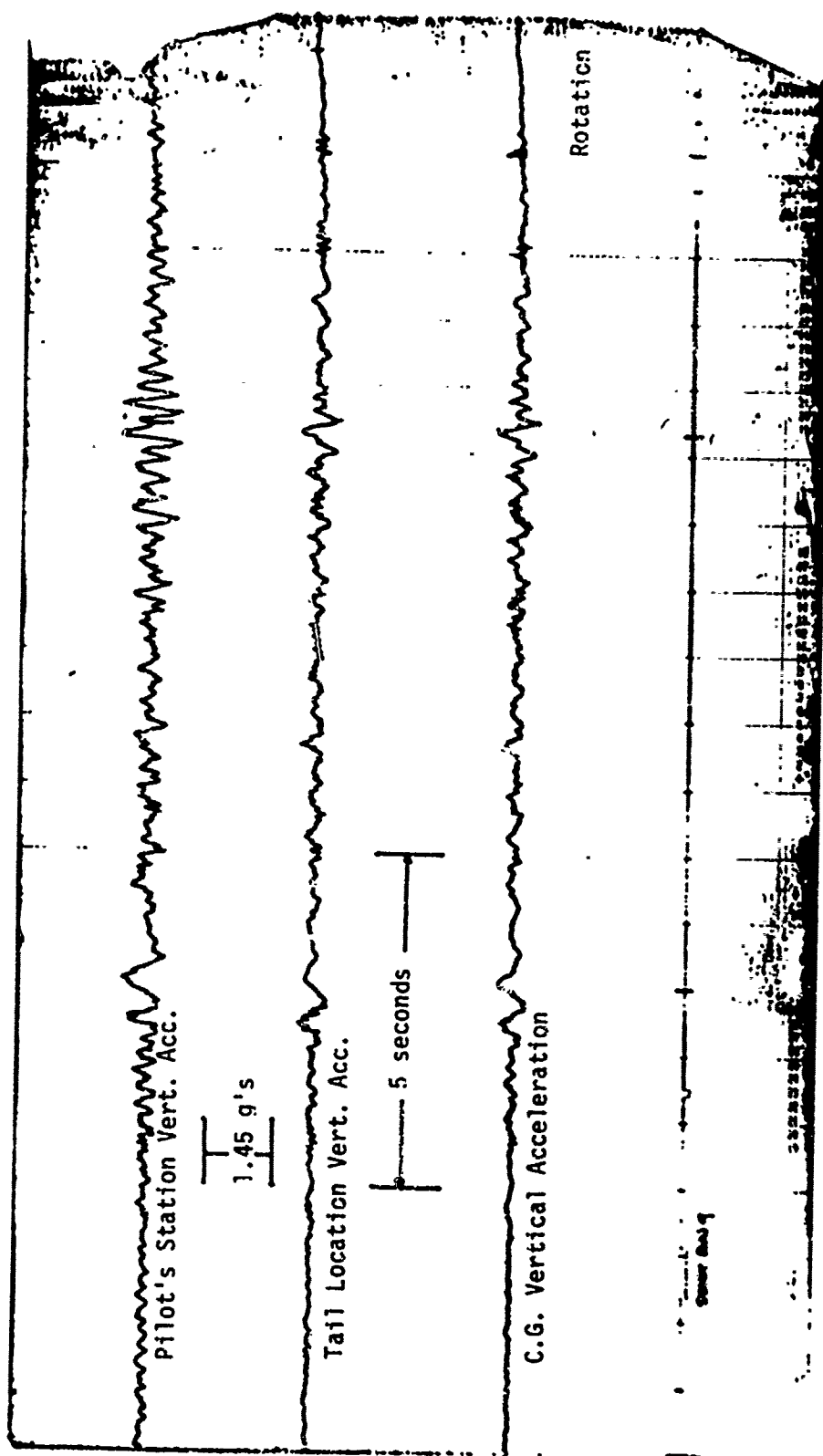


Figure 16. Measured Response of a Boeing 727-100 Takeoff at Washington National Airport Runway 36

TABLE 4  
COMPARISONS OF SIMULATED AND EXPERIMENTAL DATA

Experimental Time (sec)	P.S. Vertical Acceleration		C.G. Vertical Acceleration	
	Exp (g's)	Sim (g's)	Exp (g's)	Sim (g's)
8.0	0.9425	0.90	0.55	0.35
16.3	1.305	1.12	0.80	0.40
20.5	TAKEOFF			

Note: All measurements are measured from peak to peak.

The remaining simulations made were with the inclusion of wing flexibility in the simulations. The purpose of including the wing flexibility was to see if there was a significant change in P.S. and C.G. vertical acceleration response when the wing was permitted to bend when acted on by a main landing gear strut force. These simulations were made on the C-9A only because this was the only aircraft for which wing flexibility data was available. Figure 17 shows the plotted results of C-9A with flexible wings traversing the 1-cos dip at a 45° angle. This figure can be compared to Figure 10 which is the same simulation without flexible wings. By superimposing the two plots it was determined after T=17 seconds, small changes in vertical acceleration were appearing in both the P.S. and C.G. responses. Generally the higher accelerations occurred on the C-9A simulation with flexible wings. Also there was a phase lag. By the end of the run the rigid wing model lagged the flexible wing model by approximately one half of a cycle. Figure 18 shows the plotted response of the C-9A with flexible wings during a takeoff simulation from Washington National Runway 36. Figure 14 shows the same simulation without flexible wings. Superposition of the two plots shows little change, if any, in the airplane's response.

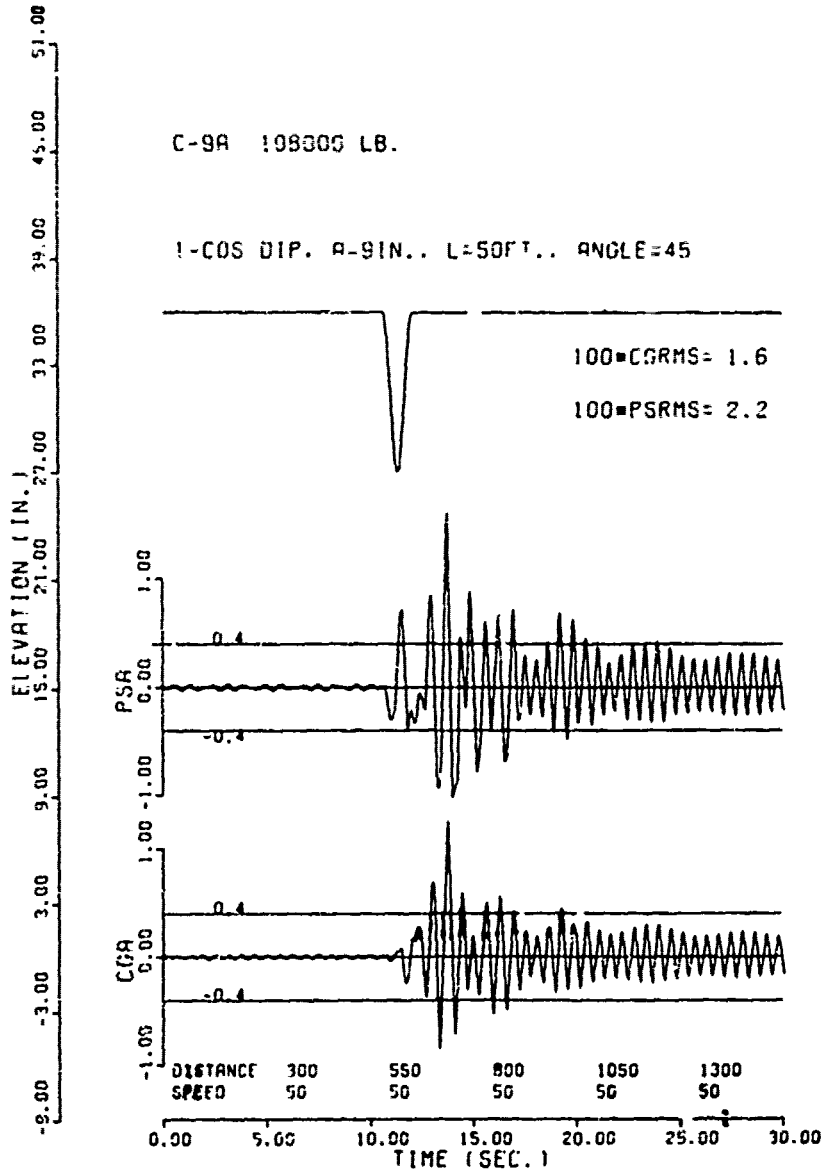


Figure 17. C-9A with Flexible Wings Taxiing over a (1-cos) dip at a 45° angle

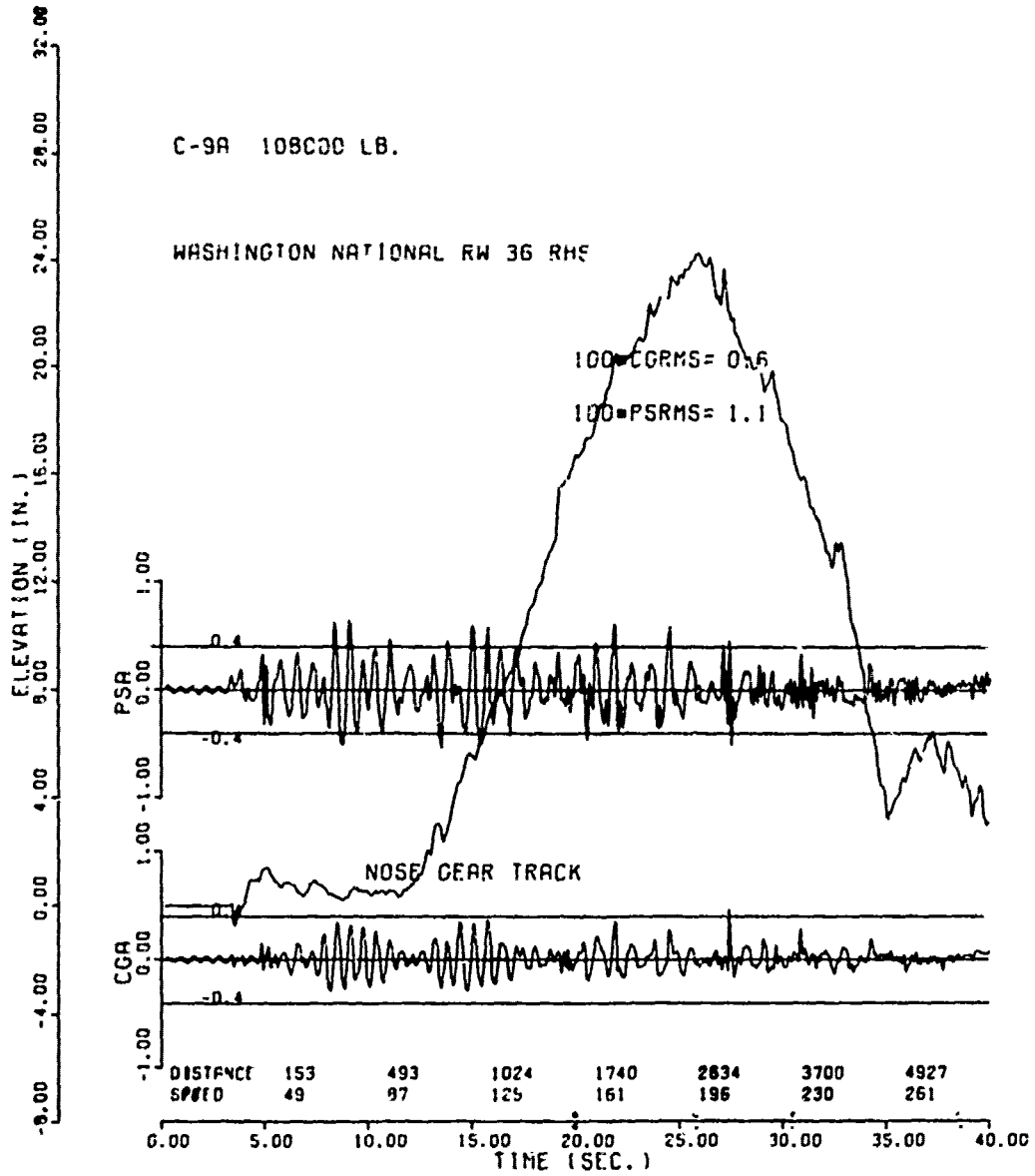


Figure 18. C-9A with Flexible Wings Taking Off from Washington National Runway 36

SECTION V  
SUMMARY AND CONCLUSIONS

In summary, a mathematical model has been formulated and programmed for a digital computer and is capable of simulating most flexible aircraft traversing an unsymmetric runway profile during constant speed taxi or takeoff. Three different aircraft have been simulated and comparisons have been made with experimental data.

Based on the 11 simulations made, the following conclusions were drawn:

1. The roll degree of freedom has a significant effect on the pilot's station and center of gravity vertical acceleration levels if the runway profile is asymmetric. The degree is dependent upon how asymmetric the profile is.

2. The effect of wing flexibility on F.S. and C.G. vertical acceleration response is small enough to be neglected, at least for the airplane simulated (C-9A). However, with the addition of flexible wings, it now becomes an easy matter to expand the computer program to obtain vertical accelerations (and consequently shears and moments) at vital wing stations such as the wing root and engine and stores pylons. This would be a natural extension of the study.

3. Comparison of the simulated aircraft response with the limited amount of available test data was satisfactory. The roughest parts of the runway were identified and, as in the test, pilot station acceleration levels exceeded the  $\pm 0.4g$  criterion. If exact strut and tire pressures, and inertia's were known for the test aircraft, the simulated C.G. response may have more closely matched the experimental data.

The simulated takeoff took an additional 5 seconds to reach rotation speed. It is assumed that the actual test aircraft weight was less than 120,000 pounds, because several runs were made without refueling the aircraft after each run. Therefore, some of the fuel had been burned off. The fact that the airplane was lighter than



that simulated would also contribute to the difference in C.G. response. Also, using a 15° flap setting changed the value of  $C_L$  and resulted in a shorter takeoff distance.

4. This computer program, "TAX2", appears to be a very efficient technique for locating the rough areas of an asymmetric runway. Using a CDC 6600 digital computer, a C-9A takeoff simulation required 70 seconds of central processor (CP) computer time, which is just 30 seconds over real time for this simulation. These numbers are typical for most simulations.

One of the advantages of a program of this type is that runway repairs can be simulated before the actual repair is made in order to determine the minimum amount of repair required. In addition, the effect of the proposed repair on other aircraft can be determined before the repair is made.

AFFDL-TR-77-37

APPENDIX A  
DEVELOPMENT OF EQUATIONS OF MOTION

Development of equations of motion using Lagrange equations. All symbols refer to Figure A-1.

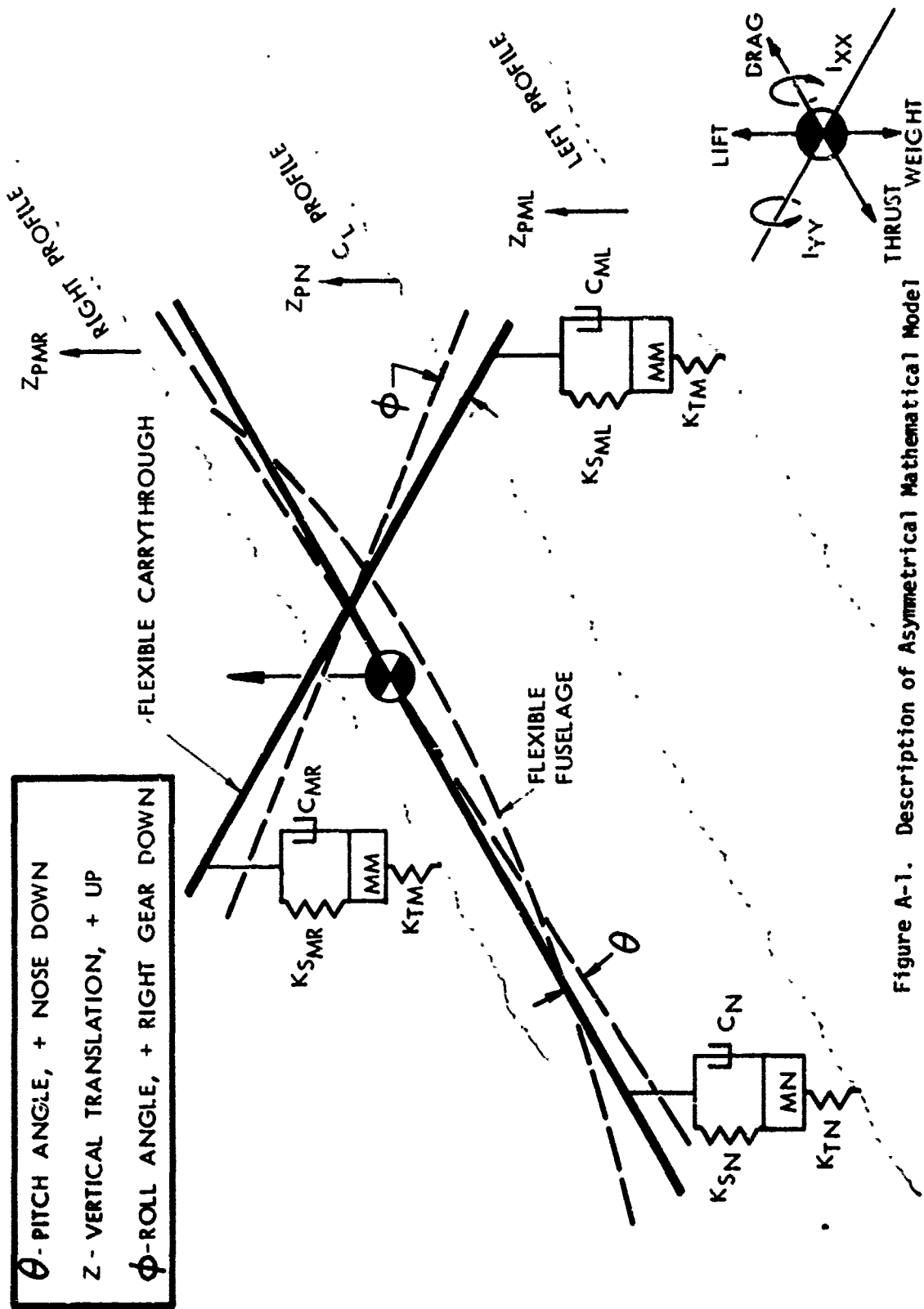


Figure A-1. Description of Asymmetrical Mathematical Model

Using Lagrange

$$\frac{d}{dt} \frac{\partial KE}{\partial \dot{q}_i} - \frac{\partial KE}{\partial q_i} + \frac{\partial PE}{\partial q_i} + \frac{\partial DE}{\partial \dot{q}_i} = 0$$

The Kinetic Energy is:

$$\begin{aligned} \text{K.E.} = & \frac{1}{2} M_{cg} \dot{z}_{cg}^2 + \frac{1}{2} M_{MR} \dot{z}_{MR}^2 + \frac{1}{2} M_{ML} \dot{z}_{ML}^2 \\ & + \frac{1}{2} M_N \dot{z}_N^2 + \frac{1}{2} I_{yy} \dot{\theta}^2 + \frac{1}{2} I_{xx} \dot{\phi}^2 \end{aligned}$$

The Potential Energy is:

$$\begin{aligned} \text{P.E.} = & + W_M z_{MR} + W_M z_{ML} + W_N z_N + W z_{cg} - L z_{cg} \\ & + \frac{1}{2} K_{SML} (z_{cg} + A\theta - z_{ML} - C\phi)^2 + \frac{1}{2} K_{T1} (z_{ML} - z_{PML})^2 \\ & + \frac{1}{2} K_{SMR} (z_{cg} + A\theta - z_{MR} + C\phi)^2 + \frac{1}{2} K_{TM} (z_{MR} - z_{PMR})^2 \\ & + \frac{1}{2} K_{SN} (z_{cg} - B\theta - z_N)^2 + \frac{1}{2} K_{TN} (z_N - z_{PN})^2 \end{aligned}$$

The Dissipative Energy is:

$$\begin{aligned} \text{D.E.} = & + \frac{1}{2} C_{ML} (\dot{z}_{cg} + A\dot{\theta} - \dot{z}_{ML} - C\dot{\phi})^2 \\ & + \frac{1}{2} C_{MR} (\dot{z}_{cg} + A\dot{\theta} - \dot{z}_{MR} + C\dot{\phi})^2 \\ & + \frac{1}{2} C_N (\dot{z}_{cg} - B\dot{\theta} - \dot{z}_N)^2 \end{aligned}$$

Now Find  $\frac{d}{dt} \frac{\partial KE}{\partial \dot{q}_i}$

$$\frac{d}{dt} \frac{\partial KE}{\partial \dot{z}_{cg}} = M \ddot{z}_{cg} ; \frac{d}{dt} \frac{\partial KE}{\partial \dot{z}_N} = M_N \ddot{z}_N$$

$$\frac{d}{dt} \frac{\partial KE}{\partial \dot{z}_{MR}} = M_{MR} \ddot{z}_{MR} ; \frac{d}{dt} \frac{\partial KE}{\partial \dot{\theta}} = I_{yy} \ddot{\theta}$$

$$\frac{d}{dt} \frac{\partial KE}{\partial \dot{z}_{ML}} = M_{ML} \ddot{z}_{ML} ; \frac{d}{dt} \frac{\partial KE}{\partial \dot{\phi}} = I_{xx} \ddot{\phi}$$

$$\frac{\partial KE}{\partial q_i} = 0$$

Now Find  $\frac{\partial(P.E)}{\partial q_i}$

---

$$\frac{\partial(P.E)}{\partial Z_{cg}} = + K_{SML}(Z_{cg} + A\theta - Z_{ML} - C\phi)$$

$$+ K_{SMR}(Z_{cg} + A\theta - Z_{MR} + C\phi)$$

$$+ K_{SN}(Z_{cg} - B\theta - Z_N) + W - L$$

$$\frac{\partial(P.E)}{\partial Z_{MR}} = + W_M - K_{SMR}(Z_{cg} + A\theta - Z_{MR} + C\phi)$$

$$+ K_{TM}(Z_{MR} - Z_{PMR})$$

$$\frac{\partial(P.E)}{\partial Z_{ML}} = + W_M - K_{SML}(Z_{cg} + A\theta - Z_{ML} - C\phi)$$

$$+ K_{TM}(Z_{ML} - Z_{PML})$$

$$\frac{\partial(P.E)}{\partial Z_N} = + W_N - K_{SN}(Z_{cg} - B\theta - Z_N) + K_{TN}(Z_N - Z_{PN})$$

$$\frac{\partial(P.E)}{\partial \theta} = + K_{SML}A(Z_{cg} + A\theta - Z_{ML} - C\phi)$$

$$+ K_{SMR}A(Z_{cg} + A\theta - Z_{MR} + C\phi)$$

$$- K_{SN}B(Z_{cg} - B\theta - Z_N)$$

$$\frac{\partial(P.E)}{\partial \phi} = - K_{SML}C(Z_{cg} + A\theta - Z_{ML} - C\phi)$$

$$+ K_{SMR}C(Z_{cg} + A\theta - Z_{MR} + C\phi)$$

Now Find  $\frac{\partial(D.E)}{\partial \dot{q}_i}$

---

$$\frac{\partial(D.E)}{\partial \dot{Z}_{MR}} = - C_{MR}(\dot{Z}_{cg} + A\dot{\theta} - \dot{Z}_{MR} + C\dot{\phi})$$

$$\frac{\partial(D.E)}{\partial \dot{z}_{ML}} = - C_{ML} (\dot{z}_{cg} + A\dot{\theta} - \dot{z}_{ML} - C\dot{\phi})$$

$$\frac{\partial(D.E)}{\partial \dot{z}_N} = - C_N (\dot{z}_{cg} - B\dot{\theta} - \dot{z}_N)$$

$$\begin{aligned} \frac{\partial(D.E)}{\partial \dot{z}_{cg}} &= + C_{MR} (\dot{z}_{cg} + A\dot{\theta} - \dot{z}_{MR} + C\dot{\phi}) \\ &\quad + C_{ML} (\dot{z}_{cg} + A\dot{\theta} - \dot{z}_{ML} - C\dot{\phi}) \\ &\quad - C_N (\dot{z}_{cg} - B\dot{\theta} - \dot{z}_N) \end{aligned}$$

$$\begin{aligned} \frac{\partial(D.E)}{\partial \dot{\theta}} &= + C_{MR} A (\dot{z}_{cg} + A\dot{\theta} - \dot{z}_{MR} + C\dot{\phi}) \\ &\quad + C_{ML} A (\dot{z}_{cg} + A\dot{\theta} - \dot{z}_{ML} - C\dot{\phi}) \\ &\quad - C_N B (\dot{z}_{cg} - B\dot{\theta} - \dot{z}_N) \end{aligned}$$

$$\begin{aligned} \frac{\partial(D.E)}{\partial \dot{\phi}} &= + C_{MR} C (\dot{z}_{cg} + A\dot{\theta} - \dot{z}_{MR} + C\dot{\phi}) \\ &\quad - C_{ML} C (\dot{z}_{cg} + A\dot{\theta} - \dot{z}_{ML} - C\dot{\phi}) \end{aligned}$$

Combine Terms

$$\begin{aligned} \ddot{Mz}_{cg} &= - K_{SML} [z_{cg} + \overset{(X_{ML})}{A\theta} - z_{ML} - C\phi] \\ &\quad - K_{SMR} [z_{cg} + \overset{(X_{MR})}{A\theta} - z_{MR} + C\phi] \\ &\quad - K_{SN} [z_{cg} - \overset{(X_N)}{B\theta} - z_N] - W + L \\ &\quad - C_{MR} [\dot{z}_{cg} + \overset{(X_{MR})}{A\dot{\theta}} - \dot{z}_{MR} + C\dot{\phi}] \\ &\quad - C_{ML} [\dot{z}_{cg} + \overset{(X_{ML})}{A\dot{\theta}} - \dot{z}_{ML} - C\dot{\phi}] \\ &\quad - C_N [\dot{z}_{cg} - \overset{(X_N)}{B\dot{\theta}} - \dot{z}_N] \end{aligned}$$

Rewriting we have

$$\ddot{Mz}_{cg} = [-K_{SML}(X_{ML}) - C_{ML}(\dot{X}_{ML})] + \quad (1)$$

$$[-K_{SMR}(x_{MR}) - C_{MR}(\dot{x}_{MR})] +$$

$$[-K_{SN}(x_N) - C_N(\dot{x}_N)] - W + L$$

where the terms in the brackets are the left, right, and nose landing gear strut forces respectively.

Similarly

$$M_M \ddot{z}_{ML} = K_{SML}(x_{ML}) + C_{ML}(\dot{x}_{ML}) \quad (2)$$

$$- K_{TM}(z_{ML} - z_{PML}) - W_M$$

$$M_M \ddot{z}_{MR} = K_{SMR}(x_{MR}) + C_{MR}(\dot{x}_{MR}) \quad (3)$$

$$- K_{TM}(z_{MR} - z_{PMR}) - W_M$$

$$M_N \ddot{z}_N = K_{SN}(x_N) + C_N(\dot{x}_N) - K_{TN}(z_N - z_{PN}) \quad (4)$$

$$I_{yy} \ddot{\theta} = -K_{SML}A(x_{ML}) + C_{ML}A(\dot{x}_{ML})$$

$$+ K_{SMR}A(x_{MR}) + C_{MR}A(\dot{x}_{MR}) \quad (5)$$

$$- K_N B(x_N) + C_N B(\dot{x}_N)$$

$$I_{xy} \ddot{\phi} = K_{SML}C(x_{ML}) + C_{ML}C(\dot{x}_{ML}) \quad (6)$$

$$- K_{SMR}C(x_{MR}) - C_{MR}C(\dot{x}_{MR})$$

The Forward Translation Equation of Motion is uncoupled and expressed as follows:

$$MX = T - D_a - D_t$$

where:

T = Thrust

D<sub>a</sub> = Aerodynamic Drag

D<sub>t</sub> = Tire Drag (Total)

The modal method will be used to express the aircraft's flexibility as follows:

$$M_i \ddot{q}_i = \xi_{ij} F_j - 2\zeta\omega_i M_i \dot{q}_i - \omega_i^2 M_i q_i$$

where  $i$  = the  $i$ th mode

$F_j$  = the  $j$ th force input into the system (such as strut force)

$M_i$  = the  $i$ th generalized mass

$q_i$  = the generalized coordinate

$\xi_{ij}$  = the modal deflection of the  $i$ th mode at fuselage station  $j$  for symmetric modes or wing station  $j$  for asymmetric modes.

$\omega_i$  = the  $i$ th mode natural frequency

$\zeta$  = Structural damping factor

By using this technique the displacements  $X'_{MR}$ ,  $X'_{ML}$ ,  $X'_N$  and their time derivatives reflect the motion of the bending fuselage and wings by adding the  $\sum_{i=1}^N q_i \xi_{ij}$  (modal displacements) at the  $j$ th (required location).

For example;

$$\text{Total Displacement } X'_{MR} = X_{MR} + \sum_{i=1}^N q_i \xi_{iR} + \sum_{k=1}^P q_k \xi_{kR}$$

$$\text{Total Velocity } \dot{X}'_{MR} = \dot{X}_{MR} + \sum_{i=1}^N \dot{q}_i \xi_{iR} + \sum_{k=1}^P \dot{q}_k \xi_{kR}$$

where:

Term 1 = Displacements of the rigid body

Term 2 = Displacements due to the symmetric modes

Term 3 = Displacements due to the asymmetric modes



AFFDL-TR-77-37

APPENDIX B  
LISTING OF COMPUTER PROGRAM TAX2



BEST AVAILABLE COPY

62 C 001 DISTANCE MAIN GEAR TO CS (INCHES)  
 C 002 DISTANCE NOSE GEAR TO CS (INCHES)  
 C 003 MASS MOMENT OF INERTIA (LB IN SEC^2)  
 C 004 MS WING STATION OF WLG (INCHES)  
 C 005 WING MASS MOMENT OF INERTIA (LB IN SEC^2)  
 C 006 PLANE AIRPLANE CENTER OF GRAVITY (INCHES)  
 C 007 PIKAW - DISTANCE OF PILOT STATION TO CG  
 C 008 TAILW - DISTANCE OF TAIL STATION TO CG  
 C 009 TARDOFF TAKE-OFF SPEED (FEET/SEC)  
 C 010 SPEED CRITICAL VEL OF AIRPLANE  
 C 011 THURST TOTAL AIRPLANE THURST  
 C 012 CLIFT COEFF.  
 C 013 CDINDIC COEFF.  
 C 014 CDINDIC CREFF.  
 C 015 WINGWEIGHT OF MAIN GEAR (LBS)  
 C 016 WINGWEIGHT OF NOSE GEAR  
 C 017 SHM - NUMBER OF MAIN GEAR STRUTS  
 C 018 SHM - NUMBER OF NOSE GEAR STRUTS  
 C 019 AMN HYDRAULIC PISTON AREA NOSE 53 INCHES  
 C 020 AMN HYDRAULIC PISTON AREA MAIN 53 INCHES  
 C 021 AMN HYDRAULIC PISTON AREA MAIN 52 INCHES  
 C 022 AMN HYDRAULIC PISTON AREA MAIN 53 INCHES  
 C 023 PCON NOSE STRUT BEFORE PRESSURE PSI  
 C 024 PCON MAIN STRUT BEFORE PRESSURE PSI  
 C 025 VON NOSE STRUT INITIAL VOLUME "3, 14,  
 C 026 VON MAIN STRUT INITIAL VOLUME "3, 14,  
 C 027 OAN ORIFACE AREA MAIN  
 C 028 OAN ORIFACE AREA NOSE  
 C 029 SLM MAIN GEAR STRUT LENGTH UNLOADED INCHES  
 C 030 SLM NOSE GEAR STRUT LENGTH UNLOADED INCHES  
 C 031 SLM NOSE GEAR STRUT LENGTH UNLOADED INCHES  
 C 032 DISTANCE FROM CL OF AXLE TO CS LINE  
 C 033 DISTANCE FROM CL OF AXLE TO CS LINE  
 C 034 DISTANCE FROM CL OF AXLE TO CS LINE  
 C 035 TSM MAIN TIRE SPRING CONSTANT PER STRUT  
 C 036 TSM NOSE TIRE SPRING CONSTANT PER STRUT  
 C 037 DRTIME STRUT SIZE DESCRIPTION STARTING AT 2:00 STROKE  
 C 038 READ METERS PER CHANGE NOSE GEAR  
 C 039 READ METERS PER CHANGE MAIN GEAR  
 C 040 WCM - NUMBER OF FLEXIBLE MODES  
 C 041 WCM - NUMBER OF ASYMMETRIC MODES  
 C 042 SIXTEX(1) - MODE SHAPE DEFLECTION (NON 314,  
 C 043 GMS) - GENERALIZED MASS (POUNDS-SEC^2/IN)  
 C 044 OMEGA (1) - MODAL FREQUENCIES (RAD/SEC)  
 C 045 SILEFT(1) - LEFT GEAR MODE SHAPE DEFLECTION  
 C 046 SIRIGHT(1) - RIGHT GEAR MODE SHAPE DEFLECTION  
 C 047 CHA(1) - ASYM, MODE NUM, MASS  
 C 048 OMEGA(1) - ASYM, MODE FREQ.  
 C 049 READ (5,11) VALUE  
 C 050 FORMAT(0410)  
 C 051 READ(5,9) L-0,0,MW,MS,MW19  
 C 052 FORMAT(6F16.1,2F12.8)  
 C 053 READ(5,10) OSAD0,TAILRM  
 C 054 FORMAT(2F10.2)  
 C 055 READ(5,11) -SPEED,THURST,TARDOFF  
 C 056 FORMAT(3F10.3)  
 C 057 READ(5,20) CL,AREA,CD  
 C 058 FORMAT(3F10.4)

BEST AVAILABLE COPY

```

105 READ(5,25) MW,OM,SM,SKN
    FORMAT(P10.2)
110 READ(5,30) AMH,AMH,AMH,ARM
    FORMAT(P10.5)
120 READ(5,35) PAOM,PAOM,VDU,VDM,CAM,DM
    FORMAT(P10.9)
130 READ(5,40) SLW,SLN
    FORMAT(P10.3)
140 READ(5,45) TSM,OTSM
    FORMAT(P10.11)
150 READ(5,50) TPL,OT,PLIST
    FORMAT(P10.3)
160 READ(5,55) WSCN
    FORMAT(I2)
170 READ(5,60) (STRC(I),I=1,N2CN)
    FORMAT(I2,10.3)
180 READ(5,65) WSCN
    FORMAT(I2,10.3)
190 READ(5,70) (STRC(I),I=1,N2CN)
    FORMAT(I2,10.3)
200 READ(5,75) (STRC(I),I=1,N2CN)
    FORMAT(I2,10.3)
210 READ(5,80) (STRC(I),I=1,N2CN)
    FORMAT(I2,10.3)
220 READ(5,85) (STRC(I),I=1,N2CN)
    FORMAT(I2,10.3)
230 READ(5,90) (STRC(I),I=1,N2CN)
    FORMAT(I2,10.3)
240 READ(5,95) (STRC(I),I=1,N2CN)
    FORMAT(I2,10.3)
250 READ(5,100) (STRC(I),I=1,N2CN)
    FORMAT(I2,10.3)
260 READ(5,105) (STRC(I),I=1,N2CN)
    FORMAT(I2,10.3)
270 READ(5,110) (STRC(I),I=1,N2CN)
    FORMAT(I2,10.3)
280 READ(5,115) (STRC(I),I=1,N2CN)
    FORMAT(I2,10.3)
290 READ(5,120) (STRC(I),I=1,N2CN)
    FORMAT(I2,10.3)
300 READ(5,125) (STRC(I),I=1,N2CN)
    FORMAT(I2,10.3)
310 READ(5,130) (STRC(I),I=1,N2CN)
    FORMAT(I2,10.3)
320 READ(5,135) (STRC(I),I=1,N2CN)
    FORMAT(I2,10.3)
330 READ(5,140) (STRC(I),I=1,N2CN)
    FORMAT(I2,10.3)
340 READ(5,145) (STRC(I),I=1,N2CN)
    FORMAT(I2,10.3)
350 READ(5,150) (STRC(I),I=1,N2CN)
    FORMAT(I2,10.3)
360 READ(5,155) (STRC(I),I=1,N2CN)
    FORMAT(I2,10.3)
370 READ(5,160) (STRC(I),I=1,N2CN)
    FORMAT(I2,10.3)
380 READ(5,165) (STRC(I),I=1,N2CN)
    FORMAT(I2,10.3)
390 READ(5,170) (STRC(I),I=1,N2CN)
    FORMAT(I2,10.3)
400 READ(5,175) (STRC(I),I=1,N2CN)
    FORMAT(I2,10.3)
410 READ(5,180) (STRC(I),I=1,N2CN)
    FORMAT(I2,10.3)
420 READ(5,185) (STRC(I),I=1,N2CN)
    FORMAT(I2,10.3)
430 READ(5,190) (STRC(I),I=1,N2CN)
    FORMAT(I2,10.3)
440 READ(5,195) (STRC(I),I=1,N2CN)
    FORMAT(I2,10.3)
450 READ(5,200) (STRC(I),I=1,N2CN)
    FORMAT(I2,10.3)
460 READ(5,205) (STRC(I),I=1,N2CN)
    FORMAT(I2,10.3)
470 READ(5,210) (STRC(I),I=1,N2CN)
    FORMAT(I2,10.3)
480 READ(5,215) (STRC(I),I=1,N2CN)
    FORMAT(I2,10.3)
490 READ(5,220) (STRC(I),I=1,N2CN)
    FORMAT(I2,10.3)
500 READ(5,225) (STRC(I),I=1,N2CN)
    FORMAT(I2,10.3)
510 READ(5,230) (STRC(I),I=1,N2CN)
    FORMAT(I2,10.3)
520 READ(5,235) (STRC(I),I=1,N2CN)
    FORMAT(I2,10.3)
530 READ(5,240) (STRC(I),I=1,N2CN)
    FORMAT(I2,10.3)
540 READ(5,245) (STRC(I),I=1,N2CN)
    FORMAT(I2,10.3)
550 READ(5,250) (STRC(I),I=1,N2CN)
    FORMAT(I2,10.3)
560 READ(5,255) (STRC(I),I=1,N2CN)
    FORMAT(I2,10.3)
570 READ(5,260) (STRC(I),I=1,N2CN)
    FORMAT(I2,10.3)
580 READ(5,265) (STRC(I),I=1,N2CN)
    FORMAT(I2,10.3)
590 READ(5,270) (STRC(I),I=1,N2CN)
    FORMAT(I2,10.3)
600 READ(5,275) (STRC(I),I=1,N2CN)
    FORMAT(I2,10.3)
610 READ(5,280) (STRC(I),I=1,N2CN)
    FORMAT(I2,10.3)
620 READ(5,285) (STRC(I),I=1,N2CN)
    FORMAT(I2,10.3)
630 READ(5,290) (STRC(I),I=1,N2CN)
    FORMAT(I2,10.3)
640 READ(5,295) (STRC(I),I=1,N2CN)
    FORMAT(I2,10.3)
650 READ(5,300) (STRC(I),I=1,N2CN)
    FORMAT(I2,10.3)
660 READ(5,305) (STRC(I),I=1,N2CN)
    FORMAT(I2,10.3)
670 READ(5,310) (STRC(I),I=1,N2CN)
    FORMAT(I2,10.3)
680 READ(5,315) (STRC(I),I=1,N2CN)
    FORMAT(I2,10.3)
690 READ(5,320) (STRC(I),I=1,N2CN)
    FORMAT(I2,10.3)
700 READ(5,325) (STRC(I),I=1,N2CN)
    FORMAT(I2,10.3)
710 READ(5,330) (STRC(I),I=1,N2CN)
    FORMAT(I2,10.3)
720 READ(5,335) (STRC(I),I=1,N2CN)
    FORMAT(I2,10.3)
730 READ(5,340) (STRC(I),I=1,N2CN)
    FORMAT(I2,10.3)
740 READ(5,345) (STRC(I),I=1,N2CN)
    FORMAT(I2,10.3)
750 READ(5,350) (STRC(I),I=1,N2CN)
    FORMAT(I2,10.3)
760 READ(5,355) (STRC(I),I=1,N2CN)
    FORMAT(I2,10.3)
770 READ(5,360) (STRC(I),I=1,N2CN)
    FORMAT(I2,10.3)
780 READ(5,365) (STRC(I),I=1,N2CN)
    FORMAT(I2,10.3)
790 READ(5,370) (STRC(I),I=1,N2CN)
    FORMAT(I2,10.3)
800 READ(5,375) (STRC(I),I=1,N2CN)
    FORMAT(I2,10.3)
810 READ(5,380) (STRC(I),I=1,N2CN)
    FORMAT(I2,10.3)
820 READ(5,385) (STRC(I),I=1,N2CN)
    FORMAT(I2,10.3)
830 READ(5,390) (STRC(I),I=1,N2CN)
    FORMAT(I2,10.3)
840 READ(5,395) (STRC(I),I=1,N2CN)
    FORMAT(I2,10.3)
850 READ(5,400) (STRC(I),I=1,N2CN)
    FORMAT(I2,10.3)
860 READ(5,405) (STRC(I),I=1,N2CN)
    FORMAT(I2,10.3)
870 READ(5,410) (STRC(I),I=1,N2CN)
    FORMAT(I2,10.3)
880 READ(5,415) (STRC(I),I=1,N2CN)
    FORMAT(I2,10.3)
890 READ(5,420) (STRC(I),I=1,N2CN)
    FORMAT(I2,10.3)
900 READ(5,425) (STRC(I),I=1,N2CN)
    FORMAT(I2,10.3)
910 READ(5,430) (STRC(I),I=1,N2CN)
    FORMAT(I2,10.3)
920 READ(5,435) (STRC(I),I=1,N2CN)
    FORMAT(I2,10.3)
930 READ(5,440) (STRC(I),I=1,N2CN)
    FORMAT(I2,10.3)
940 READ(5,445) (STRC(I),I=1,N2CN)
    FORMAT(I2,10.3)
950 READ(5,450) (STRC(I),I=1,N2CN)
    FORMAT(I2,10.3)
960 READ(5,455) (STRC(I),I=1,N2CN)
    FORMAT(I2,10.3)
970 READ(5,460) (STRC(I),I=1,N2CN)
    FORMAT(I2,10.3)
980 READ(5,465) (STRC(I),I=1,N2CN)
    FORMAT(I2,10.3)
990 READ(5,470) (STRC(I),I=1,N2CN)
    FORMAT(I2,10.3)

```

BEST AVAILABLE COPY

07/25/75 10:22:28 PAGE 6

```

PROGRAM TAXZ   76/76   OPT=1           FTM 6.5-64806
76  WRITE(16,76) (STRKMIN,MINOM(1),I=1,N5CV)
   FORMAT(76,14,'STROKE NOSE  MIN DIAMETER     //,1(3U,0.10,1))
77  WRITE(16,77) (STRKMIN,MINOM(1),I=1,N5CV)
   FORMAT(76,14,'STROKE MAIN  MIN DIAMETER     //,2(3R,10.0,3))
80  FORMAT(14,14,'MODE STOS  SMOSE0,4R,0  SIGS  SIMAIN  SITAIL
   DO 45  I=1,N5M
85  WRITE(16,80) (1,1,1,STOSIT),SMOSE(1),SIGG(1),SIMAIN(1),SITAIL(1),
   IOMEGA(1),CM(1))
86  FORMAT(16,86) /ASSYMETRICAL MODES//,1R,4MODE,5R,0,SIGG1,F,5R,
   10ZLEFTR,5R,0,CHCGAR,5R,0,GEN MASS)
   DO 40  I=1,N5M
88  WRITE(16,87) (1,1,1,STRICT(1),SILEFT(1),TIMEAR(1),CM(1))
   CONTINUE
89  FORMAT(14,15,3R,0,FIG,3,10)
90  FORMAT(16,89) 2R,12,6I2,2,2R,FIG,1)
93  C THE INITIAL MAIN GEAR POSITION INCHES
   WRITE(16,93)
95  FORMAT(16,95) /GSR,5M//***** INITIAL CONDITIONS *****
   C THE INITIAL NOSE GEAR POSITION INCHES
   C THE INITIAL C. POSITION INCHES
   C THE INITIAL STICK ANGLE DEGREES
   C THE ABOVE PARAMETERS ARE CALCULATED IN SUBROUTINE IC
   CALL ICI  ZCGI,ZMI,ZMI,PACTR)
   ZMI,ZMI
   ZMI,ZMI
205  WRITE(16,105) ZMI,ZMI,THEAT,FCGI
   FORMAT(16,99,4R,1R,ZMI,F10.1,5R,4R,ZMI,F10.1,5R,7R,THEAT,F10.6,
   10Z,ZCGI,F10.3,9E10,0.1)
   REACTN(ZMI,TSM,LSM)
   REACTN(ZMI,OTSM,LSOR)
   WRITE(16,106) ZMI,ZMI,THEAT,FCGI,REACTN,REACTM
210  FORMAT(17,17,5R,1R,4R,ZMI,F10.1,5R,3R,4R,ZMI,F10.1,5R,0,
   10Z,THEAT,F10.0)
   *****
215  C READ SUMMARY PROFILE DATA ELEV, ELEN, ELEN
   C SITE RUMMARY PROFILE AND DIRECTION
   C MISSING OR UNKNOWN ELEVATION DATA POINTS
   WRITE(16,111)
   FORMAT(11)
   DO 112  I=1,N8
   ELEV(I)=0.
   ELEN(I)=0.
220  ELEV(I)=0.
   REACT(I),SITE
   REACT(I),SITE
   REACT(I),SITE
   REACT(I),SITE
   REACT(I),SITE
   REACT(I),SITE
   REACT(I),SITE
   REACT(I),SITE
225  *****
   FORMAT(16)
   C) 5)

```

```

TAXZ1770
TAXZ1771
TAXZ1772
TAXZ1773
TAXZ1774
TAXZ1775
TAXZ1776
TAXZ1777
TAXZ1778
TAXZ1779
TAXZ1780
TAXZ1781
TAXZ1782
TAXZ1783
TAXZ1784
TAXZ1785
TAXZ1786
TAXZ1787
TAXZ1788
TAXZ1789
TAXZ1790
TAXZ1791
TAXZ1792
TAXZ1793
TAXZ1794
TAXZ1795
TAXZ1796
TAXZ1797
TAXZ1798
TAXZ1799
TAXZ1800
TAXZ1801
TAXZ1802
TAXZ1803
TAXZ1804
TAXZ1805
TAXZ1806
TAXZ1807
TAXZ1808
TAXZ1809
TAXZ1810
TAXZ1811
TAXZ1812
TAXZ1813
TAXZ1814
TAXZ1815
TAXZ1816
TAXZ1817
TAXZ1818
TAXZ1819
TAXZ1820
TAXZ1821
TAXZ1822
TAXZ1823
TAXZ1824
TAXZ1825
TAXZ1826
TAXZ1827
TAXZ1828
TAXZ1829
TAXZ1830
TAXZ1831
TAXZ1832
TAXZ1833
TAXZ1834
TAXZ1835
TAXZ1836
TAXZ1837
TAXZ1838
TAXZ1839
TAXZ1840
TAXZ1841
TAXZ1842
TAXZ1843
TAXZ1844
TAXZ1845
TAXZ1846
TAXZ1847
TAXZ1848
TAXZ1849
TAXZ1850
TAXZ1851
TAXZ1852
TAXZ1853
TAXZ1854
TAXZ1855
TAXZ1856
TAXZ1857
TAXZ1858
TAXZ1859
TAXZ1860
TAXZ1861
TAXZ1862
TAXZ1863
TAXZ1864
TAXZ1865
TAXZ1866
TAXZ1867
TAXZ1868
TAXZ1869
TAXZ1870
TAXZ1871
TAXZ1872
TAXZ1873
TAXZ1874
TAXZ1875
TAXZ1876
TAXZ1877
TAXZ1878
TAXZ1879
TAXZ1880
TAXZ1881
TAXZ1882
TAXZ1883
TAXZ1884
TAXZ1885
TAXZ1886
TAXZ1887
TAXZ1888
TAXZ1889
TAXZ1890
TAXZ1891
TAXZ1892
TAXZ1893
TAXZ1894
TAXZ1895
TAXZ1896
TAXZ1897
TAXZ1898
TAXZ1899
TAXZ1900
TAXZ1901
TAXZ1902
TAXZ1903
TAXZ1904
TAXZ1905
TAXZ1906
TAXZ1907
TAXZ1908
TAXZ1909
TAXZ1910
TAXZ1911
TAXZ1912
TAXZ1913
TAXZ1914
TAXZ1915
TAXZ1916
TAXZ1917
TAXZ1918
TAXZ1919
TAXZ1920
TAXZ1921
TAXZ1922
TAXZ1923
TAXZ1924
TAXZ1925
TAXZ1926
TAXZ1927
TAXZ1928
TAXZ1929
TAXZ1930
TAXZ1931
TAXZ1932
TAXZ1933
TAXZ1934
TAXZ1935
TAXZ1936
TAXZ1937
TAXZ1938
TAXZ1939
TAXZ1940
TAXZ1941
TAXZ1942
TAXZ1943
TAXZ1944
TAXZ1945
TAXZ1946
TAXZ1947
TAXZ1948
TAXZ1949
TAXZ1950
TAXZ1951
TAXZ1952
TAXZ1953
TAXZ1954
TAXZ1955
TAXZ1956
TAXZ1957
TAXZ1958
TAXZ1959
TAXZ1960
TAXZ1961
TAXZ1962
TAXZ1963
TAXZ1964
TAXZ1965
TAXZ1966
TAXZ1967
TAXZ1968
TAXZ1969
TAXZ1970
TAXZ1971
TAXZ1972
TAXZ1973
TAXZ1974
TAXZ1975
TAXZ1976
TAXZ1977
TAXZ1978
TAXZ1979
TAXZ1980
TAXZ1981
TAXZ1982
TAXZ1983
TAXZ1984
TAXZ1985
TAXZ1986
TAXZ1987
TAXZ1988
TAXZ1989
TAXZ1990
TAXZ1991
TAXZ1992
TAXZ1993
TAXZ1994
TAXZ1995
TAXZ1996
TAXZ1997
TAXZ1998
TAXZ1999
TAXZ2000
TAXZ2001
TAXZ2002
TAXZ2003
TAXZ2004
TAXZ2005
TAXZ2006
TAXZ2007
TAXZ2008
TAXZ2009
TAXZ2010
TAXZ2011
TAXZ2012
TAXZ2013
TAXZ2014
TAXZ2015
TAXZ2016
TAXZ2017
TAXZ2018
TAXZ2019
TAXZ2020
TAXZ2021
TAXZ2022
TAXZ2023
TAXZ2024
TAXZ2025
TAXZ2026
TAXZ2027
TAXZ2028
TAXZ2029
TAXZ2030
TAXZ2031
TAXZ2032
TAXZ2033
TAXZ2034
TAXZ2035
TAXZ2036
TAXZ2037
TAXZ2038
TAXZ2039
TAXZ2040
TAXZ2041
TAXZ2042
TAXZ2043
TAXZ2044
TAXZ2045
TAXZ2046
TAXZ2047
TAXZ2048
TAXZ2049
TAXZ2050
TAXZ2051
TAXZ2052
TAXZ2053
TAXZ2054
TAXZ2055
TAXZ2056
TAXZ2057
TAXZ2058
TAXZ2059
TAXZ2060
TAXZ2061
TAXZ2062
TAXZ2063
TAXZ2064
TAXZ2065
TAXZ2066
TAXZ2067
TAXZ2068
TAXZ2069
TAXZ2070
TAXZ2071
TAXZ2072
TAXZ2073
TAXZ2074
TAXZ2075
TAXZ2076
TAXZ2077
TAXZ2078
TAXZ2079
TAXZ2080
TAXZ2081
TAXZ2082
TAXZ2083
TAXZ2084
TAXZ2085
TAXZ2086
TAXZ2087
TAXZ2088
TAXZ2089
TAXZ2090
TAXZ2091
TAXZ2092
TAXZ2093
TAXZ2094
TAXZ2095
TAXZ2096
TAXZ2097
TAXZ2098
TAXZ2099
TAXZ2100
TAXZ2101
TAXZ2102
TAXZ2103
TAXZ2104
TAXZ2105
TAXZ2106
TAXZ2107
TAXZ2108
TAXZ2109
TAXZ2110
TAXZ2111
TAXZ2112
TAXZ2113
TAXZ2114
TAXZ2115
TAXZ2116
TAXZ2117
TAXZ2118
TAXZ2119
TAXZ2120
TAXZ2121
TAXZ2122
TAXZ2123
TAXZ2124
TAXZ2125
TAXZ2126
TAXZ2127
TAXZ2128
TAXZ2129
TAXZ2130
TAXZ2131
TAXZ2132
TAXZ2133
TAXZ2134
TAXZ2135
TAXZ2136
TAXZ2137
TAXZ2138
TAXZ2139
TAXZ2140
TAXZ2141
TAXZ2142
TAXZ2143
TAXZ2144
TAXZ2145
TAXZ2146
TAXZ2147
TAXZ2148
TAXZ2149
TAXZ2150
TAXZ2151
TAXZ2152
TAXZ2153
TAXZ2154
TAXZ2155
TAXZ2156
TAXZ2157
TAXZ2158
TAXZ2159
TAXZ2160
TAXZ2161
TAXZ2162
TAXZ2163
TAXZ2164
TAXZ2165
TAXZ2166
TAXZ2167
TAXZ2168
TAXZ2169
TAXZ2170
TAXZ2171
TAXZ2172
TAXZ2173
TAXZ2174
TAXZ2175
TAXZ2176
TAXZ2177
TAXZ2178
TAXZ2179
TAXZ2180
TAXZ2181
TAXZ2182
TAXZ2183
TAXZ2184
TAXZ2185
TAXZ2186
TAXZ2187
TAXZ2188
TAXZ2189
TAXZ2190
TAXZ2191
TAXZ2192
TAXZ2193
TAXZ2194
TAXZ2195
TAXZ2196
TAXZ2197
TAXZ2198
TAXZ2199
TAXZ2200
TAXZ2201
TAXZ2202
TAXZ2203
TAXZ2204
TAXZ2205
TAXZ2206
TAXZ2207
TAXZ2208
TAXZ2209
TAXZ2210
TAXZ2211
TAXZ2212
TAXZ2213
TAXZ2214
TAXZ2215
TAXZ2216
TAXZ2217
TAXZ2218
TAXZ2219
TAXZ2220
TAXZ2221
TAXZ2222
TAXZ2223
TAXZ2224
TAXZ2225
TAXZ2226
TAXZ2227
TAXZ2228
TAXZ2229
TAXZ2230
TAXZ2231
TAXZ2232
TAXZ2233
TAXZ2234
TAXZ2235
TAXZ2236
TAXZ2237
TAXZ2238
TAXZ2239
TAXZ2240
TAXZ2241
TAXZ2242
TAXZ2243
TAXZ2244
TAXZ2245
TAXZ2246
TAXZ2247
TAXZ2248
TAXZ2249
TAXZ2250
TAXZ2251
TAXZ2252
TAXZ2253
TAXZ2254
TAXZ2255
TAXZ2256
TAXZ2257
TAXZ2258
TAXZ2259
TAXZ2260
TAXZ2261
TAXZ2262
TAXZ2263
TAXZ2264
TAXZ2265
TAXZ2266
TAXZ2267
TAXZ2268
TAXZ2269
TAXZ2270

```

BEST AVAILABLE COPY

```

230 117  L50 = L0 + 9
      READ(2,10) (ELEV(I), I=L0,L50)
      READ(3,10) (ELEV(I), I=L0,L50)
      READ(4,10) (ELEV(I), I=L0,L50)
      FORMAT(10F7.3)
      M13=0
      I0=L50-66-INT(S3) GO TO 124
      L0=L0+10
      GO TO 117
      ELEV1=ELEV(911)
      ELEV2=ELEV(911)
      ELEV3=ELEV(911)
      DO 125 I=91,918
      ELEV(I) = (ELEV(I)-ELEV2)*12.0
      ELEV(I) = (ELEV(I)-ELEV3)*12.0
      ELEV(I) = (ELEV(I)-ELEV1)*12.0
      DISTANCE=0
      L50=L50-9
      SLP=(L50-S91)*2
      SLP=ELEV(L50)/SLP
      DO 126 I=91, 918
      ELEV(I) =ELEV(I) -SLP*DISTAN
      ELEV(I)=ELEV(I)-SLP*DISTAN
      ELEV(I)=ELEV(I)-SLP*DISTAN
      IVAL=(I-91)/26.
      WRITE(6,130)
      FORMAT(1H,SL, RUMWAY PROFILE DATA UNCALCULATED (SLOPE REQUIRED)
      150H,PREY DOWN THE RUMWAY)
      WRITE(6,1) SIZE
      L01=L1
      L501 = L01 + 9
      LPR24 = L501 + 7
      WRITE(6,140) (ELEV(I), I=L01,L501) ,LPR24
      FORMAT(13H,10.9,107,10)
      L01=L01+10
      IF (L01-GE-M10) GO TO 145
      GO TO 135
      WRITE(6,150) L01
      FORMAT(12H,10.9,107,10)
      DO 161 I=L01,160
      WRITE(6,162) ELEV(I), ELEV(I), ELEV(I)
      FORMAT (16F10.9)
      ENDRUN = INT(S502)
      MM=(ENDRUN-100)/2100F.
      MM=(11*ENDRUN-100)/2100F.
      ENDRUN=ENDRUN-99.
      T(2) =ZCGI
      T(3) = 0.
      T(4) = ZMEL
      T(5) = ZMIE
      T(6)=0.
      T(7)=0.
      T(8) = ZMI
      T(9) = 0.
      T(10) = TMCZAI
      T(11) = 0.

```







BEST AVAILABLE COPY

PROGRAM TA2Z 74774 OPT:1 FPM 4.54466 09/25/76 10:22:70 PAGE 0

```

000 244LEVEL*7
    GO TO 160
    745 CONTINUE
    C  IP(10).GT.600.0) GO TO 185
    IP(10).LT.(17*MM) GO TO 240
    GO TO 165
    240 WRITE(6,255)
    255 FORMAT(9X,'THE VEHICLE HAS TAKEN OFF')
    260 WRITE(6,261) (ZKUM(I),I=1)
    262 FORMAT(13X,'END OF SUMMARY',F10.3)
    263 GO TO 1
    264 PSUMS=0.
    CCMS=0.
    DO 265 I=1,MM
    265 CCMS=CCMS+CCACC(I)*100
    PSUMS=PSUMS+SACC(I)*100
    266 PSUMS=PSUMS+ZKUM(I)*FLOOR(ZLL)
    CCMS=100.-ZKUM(I)*ZKUM(I)*FLOOR(ZLL)
    WRITE(6,266) PSUMS,CCMS
    266 FORMAT(17F20.10,'PSUMS',F10.3,'100',F10.3,'100',F10.3,'100',F10.3)
    IF(17*MM.EQ.1) GO TO 245
    ZLMS = FLOOR(INCH)/5.
    WRITE(6,267) MM,ZLL
    267 FORMAT(22I0)
    IF(MM.LE.1000) OR(LL.LT.1000) GO TO 245
    267 FORMAT(35X,'THE ARRAYS CSACC OR PSACC OR PROF 44VF EXCEEDED
    268 1 THEIR DIMENSIONED SIZE')
    CONTINUE
    CALL FACTOR (7,0)
    CALL PL0T(0,0,-11.0,-3)
    CALL PL0T(3,0,-7,-3)
    TIME(MM*2) = 0.0
    TIME(MM*2) = 5.0
    TIME(11*2) = 5.0
    TIME(11*2) = 5.0
    CCACC(MM*2) = 1.0
    CCACC(MM*2) = 1.0
    PSACC(11*2) = -1.0
    PSACC(11*2) = 1.0
    CALL SCALE(MM*2,10,MM,1)
    PROF(10,0,10,0) = 0.0
    PROF(10,21) = 0.0
    PROF(MM*2) = 0.0
    PROF(MM*2) = 0.0
    MM 249 101,MM
    WRITE(6,269)
    269 CALL ANTS(1,0,11*TIME (SEC),1,11,EL,305,0.0,TIME(MM*2),
    270 11*MM)
    270 WRITE(6,270)
    CALL PL0T (21,MM,11,0)
    CALL PL0T (21,MM,11,0)
    CALL SYMBOL (11,105,300)SYMS(0,0,0)
    CALL SYMBOL (11,105,300)SYMS(10,0,0)
    DO 275 I=1,11*MM
  
```

```

2426000
2426010
2426020
2426030
2426040
2426050
2426060
2426070
2426080
2426090
2426100
2426110
2426120
2426130
2426140
2426150
2426160
2426170
2426180
2426190
2426200
2426210
2426220
2426230
2426240
2426250
2426260
2426270
2426280
2426290
2426300
2426310
2426320
2426330
2426340
2426350
2426360
2426370
2426380
2426390
2426400
2426410
2426420
2426430
2426440
2426450
2426460
2426470
2426480
2426490
2426500
2426510
2426520
2426530
2426540
2426550
2426560
2426570
2426580
2426590
2426600
  
```

BEST AVAILABLE COPY

PROGRAM LIST 74/74 OPT=1 RTN 6,5,0,6,6,6 PAGE 4

```

680      CALL NUMBER(1,TIME(1),2,0,195,55,PL,OT(1),0,0,-1)
681      CALL PLOT (X,OMG,1,5,3)
682      CALL PLOT (0,0,1,5,2)
683      DO 200 I=1,177
684      CALL SYMBOL (X,OMG(1),1,0,0,5,16,6,0,1)
685      CALL PLOT (X,OMG,1,9,3)
686      CALL PLOT (0,0,1,9,2)
687      CALL SYMBOL (0,0,0,0,16,PL,AMF,9,0,0)
688      CALL SYMBOL (0,0,0,0,16,SI,EG,0,0,0)
689      CALL SYMBOL (0,0,0,0,16,SI,EG,0,0,0)
690      CALL SYMBOL (0,0,0,0,16,SI,EG,0,0,0)
691      CALL NUMBER(1,5,37,0,16,CGMS,0,1)
692      CALL NUMBER(1,5,6,5,16,CGMS,0,1)
693      X,OMG=H,OMG/2
694      CALL SYMBOL (X,OMG,2,0,5,16,11,AMF,DL,0,15,7,0,1)
695      CALL SYMBOL (X,OMG,2,0,5,16,11,AMF,DL,0,15,7,0,1)
696      CALL PLOT (1,1,3,-3)
697      CALL AXIS (0,1,3,CGC,3,2,0,90,CGC,(X,0,1),CGC,(X,0,1))
698      CALL NUMBER(1,0,0,0,185,0,0,10,0,1)
699      CALL NUMBER(1,0,5,0,0,185,0,0,10,0,1)
700      CALL PLOT (1,0,1,0,-3)
701      CALL LINE (TIME,CGC,CGC,MM,1,0,7,1)
702      CALL PLOT (X,OMG,3,1,3)
703      CALL PLOT (0,0,3,1,2)
704      CALL AXIS (0,1,3,3MPS,3,2,0,90,0,0,0,0,0,0,0,0,1)
705      CALL PLOT (X,OMG,0,1,7)
706      CALL PLOT (X,OMG,0,3)
707      CALL PLOT (X,OMG,0,2)
708      CALL NUMBER(1,0,0,0,195,0,0,0,0,0,1)
709      CALL NUMBER(1,0,0,0,195,0,0,0,0,0,1)
710      CALL PLOT (0,0,1,0,-3)
711      CALL LINE (TIME,1,5,CGC,LL,0,0,7,1)
712      CALL PLOT (1,0,3,0,-3)
713      CALL AXIS (1,0,0,0,15,ELEVATION (1,4),15,14,0,97,0,0,PM,PF (MM,1),
714      1,PM,PF (MM,2))
715      CALL PLOT (1,0,0,-3)
716      X,PM,PF=250,ABS (PM,PF (MM,1))/PM,PF (MM,2)
717      CALL SYMBOL (2,2,PM,PF,16,15,HOUSE GEAR TRACK,0,0,15)
718      CALL LINE (TIME,PM,PF,MM,1,0,7,1)
719      XSTOP=X,LOW,0,5
720      CALL PLOT (XSTOP,0,0,-3)
721      WRITE (6,2,98)
722      CALL PLOT (XSTOP,0,0,-3)
723      STOP
724      FORMAT (F50)
725      END

```

```

7426878
7426879
7426880
7426881
7426882
7426883
7426884
7426885
7426886
7426887
7426888
7426889
7426890
7426891
7426892
7426893
7426894
7426895
7426896
7426897
7426898
7426899
7426900
7426901
7426902
7426903
7426904
7426905
7426906
7426907
7426908
7426909
7426910
7426911
7426912
7426913
7426914
7426915
7426916
7426917
7426918
7426919
7426920
7426921
7426922
7426923
7426924
7426925
7426926
7426927
7426928
7426929
7426930
7426931
7426932
7426933
7426934
7426935
7426936
7426937
7426938
7426939
7426940
7426941
7426942
7426943
7426944
7426945
7426946
7426947
7426948
7426949
7426950
7426951
7426952
7426953
7426954
7426955

```







BEST AVAILABLE COPY

SUBROUTINE CO 76/74 OPT=1 FTN 4,542406 05/25/76 10.22.20 PAGE 1

```

1      SUBROUTINE COEFF (Y, X, A, C, D)
2      DIMENSION Y(4)
3      CALL Y(1)
4      C = (96.0*Y(1)+96.0*Y(2)-64.0*Y(3)+4.0*Y(4))/(-128.0)
5      D = (-16.0*Y(1)+12.0*Y(2)+15.0*Y(3)-6.0*Y(4))/(-128.0)
6      RETURN
7      END

```

SUBROUTINE TL\_0K 76/74 OPT=1 FTN 4,542406 05/25/76 10.22.20 PAGE 1

```

1      SUBROUTINE TL_0K (X, SLOPE, YCEPT, S, D, N)
2      DIMENSION S(10), P(10)
3      THIS IS A 2 DIMENSIONAL TABLE LOOK UP ROUTINE
4      WITH LINEAR INTERPOLATION
5      X IS THE CURRENT VALUE OF STROKE
6      SLOPE AND YCEPT ARE CALCULATED AND RETURNED
7      S AND D MAKE UP THE TABLE
8      N IS THE NUMBER OF VALUES IN THE TABLE
9      DO I=1,N
10         IF (X-GE-S(I)).AND.(X-LE-S(I+1)).GO TO 2
11         CONTINUE
12         SLOPE = (P(I+1)-P(I))/(S(I+1)-S(I))+.01
13         YCEPT = P(I)-SLOPE*S(I)
14         RETURN
15      END

```

AFFDL-TR-77-37

APPENDIX C  
LISTING OF AIRPLANE DATA

- Boeing 727-100
- McDonnell Douglas C-9A
- AMST

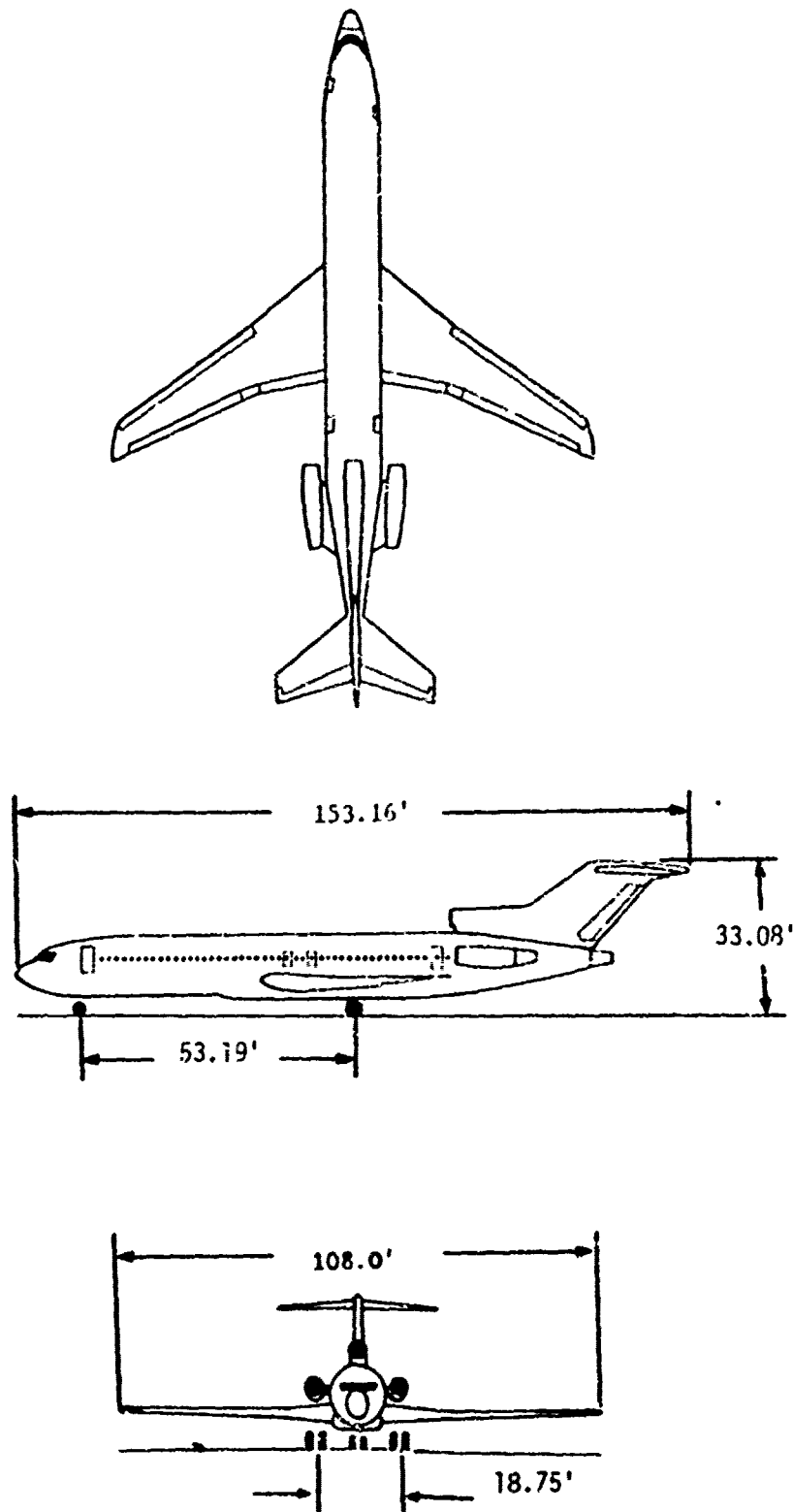


Figure C-1. Three View of Boeing 727-100



BEST AVAILABLE COPY

..... INP 7 DATA .....

..... GENERAL RECEIPT DATA .....

JOELING 727-130 1447 17 000000

MR	14660800	MR	131311	MR	699.00	AR	70.00	MR	568.700	MR	30453300.
SR	2.00	SR	1.00	SL	332.00	SL	134.00	PS	645.00	TA	211.1
AR	52.20	AR	03.00	OR	293.00	MR	732.00	OR	1.77	TS	22740.00
AR	19.00	AR	10.00	OR	253.00	VC	223.00	OR	.95	TS	0594.00
CL	0.00	CV	0.00	AR	194.00	OR	50.00	IND	10000.	TA	252.00

STRONG NOISE 314 3180000

2.220	0.00
2.440	0.00
1.000	1.000
1.000	1.000
1.000	1.000
1.000	1.000

STRONG MAIN 314 3180000

7.000	1.000
1.000	1.000
1.000	1.000
1.000	1.000

BEST AVAILABLE COPY

MODE	SIGS	SINDSF	SIGI	SIMAIN	SITAIL	OMEGA	GEN. MASS
1	-0.23	-0.23	-0.72	-0.33	-0.04	14.08	6.6
2	0.25	0.22	-0.74	-0.29	-0.06	22.97	7.0
3	-0.17	-0.19	0.02	0.00	-0.04	34.35	2.7
4	-0.23	-0.15	0.11	0.09	0.02	44.55	11.1
5	0.32	0.21	-0.71	-0.71	-0.02	49.11	1.9
6	0.21	0.16	0.25	0.33	0.08	54.66	5.0
7	-0.15	-0.04	-0.14	-0.34	0.03	75.56	1.6
8	0.33	0.10	-0.12	-0.10	-0.04	82.63	171.9
9	0.00	0.13	-0.74	-0.05	-0.03	47.85	25.1
10	-0.05	-0.13	-0.74	-0.07	-0.06	9.74	11.5

..... INITIAL CONDITIONS .....

ZMR -0.11; PMS -1.079; IMEFA -0.05792; ZCCL -13.573  
 TMAIR -17.800; PVOSS -5.423; PICTM -1614.0; PFACTM -109851.

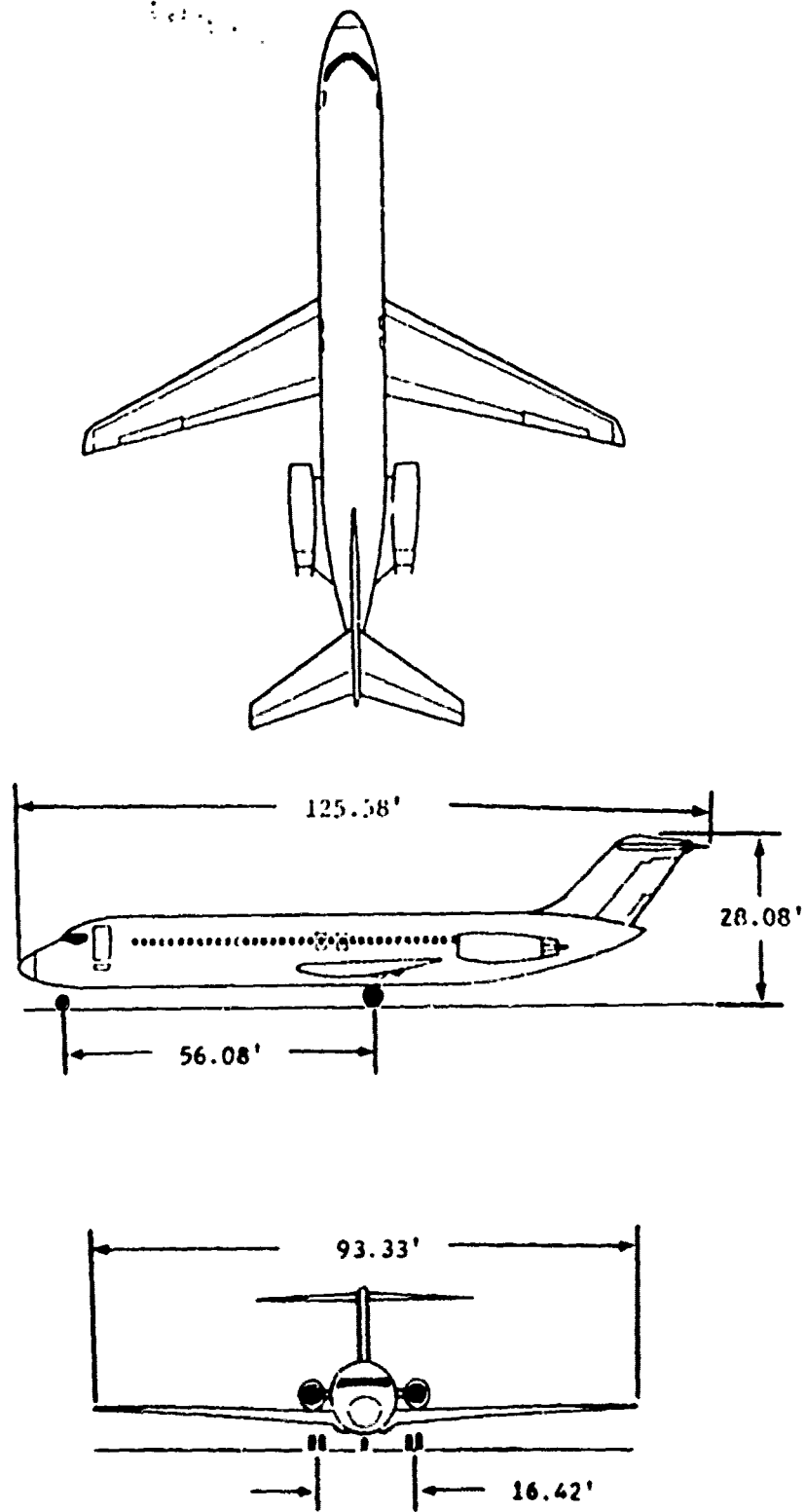


Figure C-2. Three View of McDonnell-Douglas C-9A

BEST AVAILABLE COPY

..... INPUT DATA .....

..... AIRCRAFT DATA .....

6-68 Job... 40.

NO Job... 40 577.7h 400 11.400 40 21.010 96.000 26000000.  
 NAME Sh... ..  
 Size 40 5200 300 5.000 09.5 31.00 07.5 PSARRS 007.0 FALLAMA 310.5  
 AARS 11001 000 18.000 10000 22.000 1000 500.00 0000 000 000 \* 23-20.67  
 Code 0030 0000 0000 0000 0000 0000 0000 000 000 000 \* 0032.40  
 Cto 1010 00 000 000 000 000 000 000 000 000 000 000 000 000 000 000 000 000 000 000 000  
 STRUC MDS. PIN CLAR.T...  
 0000 000 000  
 7000 000 000  
 1200 000 000  
 1300 000 000

STRUC PIN PIN CLAR.T...

0000 000 000  
 0000 000 000  
 0000 000 000  
 0000 000 000

BEST AVAILABLE COPY

MODE	SIGNUM	SCALE	EXPO	CHAR	DATA	UNIT	DESC
1	0.5	0.5	0.0	0.00	10.00	0.00	0.2
2	0.8	0.7	0.00	0.02	20.10	1.00	1.0
3	0.6	0.00	0.0	0.0	15.70	21.0	0.0
4	0.13	0.12	0.0	0.0	0.00	0.00	0.0
5	0.00	0.0	0.0	0.0	0.00	0.00	0.0
6	0.0	0.5	0.0	0.02	0.00	0.00	0.0
7	0.00	0.1	0.0	0.0	0.00	0.00	0.0

MODE	SIGNUM	SCALE	EXPO	CHAR	DATA	UNIT	DESC
1	0.02	0.0	0.0	0.0	0.00	0.00	0.0
2	0.1	0.0	0.0	0.0	0.00	0.00	0.0
3	0.02	0.0	0.0	0.0	0.00	0.00	0.0
4	0.02	0.0	0.0	0.0	0.00	0.00	0.0
5	0.00	0.0	0.0	0.0	0.00	0.00	0.0
6	0.01	0.0	0.0	0.0	0.00	0.00	0.0
7	0.02	0.0	0.0	0.0	0.00	0.00	0.0

\*\*\*\*\* INITIAL CONDITIONS \*\*\*\*\*  
 ZONE -0.117 ZONE -0.117 INITIAL -0.117 ZONE -17.21031846.  
 ANGLE -0.0017 ANGLE -0.0017 RADIAN -0.0017 RADIAN -0.0017

```

***** GENERAL APPROPRIATE DATA *****
ANST 180000.0
M 180000.0 400 1177.77  WIR  438.22  Ar  23.513  72  427.522  WIR  113.221  WIR  25350033.
44300 1592110.

```

```

SRM  2.0  544  1.3  5.44  10.0  SLUR  172.4  PSADMR  734.2  TABLE  10.2
4000 70.09  4.44  50.61  21000  53.44  VCMR  1081.01  73MR  2.72  75M  3.0000.01
4000 23.75  3.44  14.07  21000  167.33  VDMR  70.402  62MR  0.54  75M  11663.01
CL  2.650  7.3  0.651  20240  1740.01  544E0  2.0  140510  403.66  784477  178.22

```

STOGE NOSE MIN DIAMETER

6.000	0.75
6.788	0.75
6.828	0.82
11.270	0.82
16.000	0.75

STOGE MAIN MIN DIAMETER

6.000	1.200
6.788	1.278
6.828	1.200
11.270	1.278
16.000	1.200
16.000	1.278
22.000	1.278
25.000	1.278
28.000	1.278
99.271	1.278

BEST AVAILABLE COPY

CODE	STEP	START	END	START	END	START	END
1	0012	0015	0020	0020	0025	0025	0030
2	0002	0022	0025	0025	0030	0030	0035
3	0002	0025	0030	0030	0035	0035	0040
4	0026	0025	0030	0030	0035	0035	0040
5	0009	0034	0036	0036	0041	0041	0046
6	0020	0032	0035	0035	0040	0040	0045
7	0026	0030	0035	0035	0040	0040	0045
8	0006	0037	0040	0040	0045	0045	0050
9	0011	0039	0042	0042	0047	0047	0052
10	0019	0043	0046	0046	0051	0051	0056
11	0024	0047	0050	0050	0055	0055	0060
12	0027	0052	0055	0055	0060	0060	0065
13	0031	0056	0059	0059	0064	0064	0069
14	0005	0059	0062	0062	0067	0067	0072
15	0026	0063	0066	0066	0071	0071	0076

.....

.....

APPENDIX D  
LISTING OF RUNWAY PROFILES

1. Figure D-1 - Washington National Runway 36-Left, Center, and Right hand profiles:
2. Profile data listing of the 1-cos dip used in these simulations:  
All three lines of profile were identical except that they occur at different times corresponding to the gear locations.



Figure D-1. Washington National Runway 36 with Linear Truss and Removed

# BEST AVAILABLE COPY

0-11 1000 100 00000

[The main body of the page contains several large blocks of text that are extremely faint and illegible. The text appears to be organized into paragraphs, but the individual characters and words cannot be discerned.]

BIBLIOGRAPHY

Butterworth, C. K., and Boozer, D. E., Jr., C-141A Computer Code for Runway Roughness Studies, AFWL-TR-70-71, Air Force Weapons Laboratory, Kirtland AFB, New Mexico, August 1970.

Chance Vought Corporation, A Rational Method for Predicting Alighting Gear Dynamic Loads, ASD-TDR-62-555, Aeronautical Systems Division, Wright-Patterson AFB, Ohio, December 1963.

Cook, Robert F., Use of Discrete Runway Profile Elevation Data in Determining the Dynamic Response of Vehicles, TM-68-3-FDDS, Air Force Flight Dynamics Laboratory, Wright-Patterson AFB, Ohio, May 1968.

Crenshaw, B. M., and Butterworth, C. K., Lockheed Georgia Company, Aircraft Landing Gear Dynamic Loads from Operation on Clay and Sandy Soil, AFFDL-TR-69-51, Air Force Flight Dynamics Laboratory, Wright-Patterson AFB, Ohio, February 1971.

NACA TN 2477, Investigation of the Air-Compression Process During Drop Tests of an Oleo-Pneumatic Landing Gear, 1951.

Quade, Delmar A., The Boeing Company, Wichita Division, Location of Rough Areas of Runways for B-52 Aircraft, AFFDL-TR-67-175, Air Force Flight Dynamics Laboratory, Wright-Patterson AFB, Ohio, March 1968.

REFERENCES

1. Goldman, D. E., and von Gierke, H. E., "Effects of Shock and Vibration on Man," Volume III, Chap. 44, Shock and Vibration Handbook (C. M. Harris and C. E. Crede, editors) McGraw Hill Book Co., New York, 1961.
2. Gerardi, A. G., Lohwasser, A. K., Computer Program for the Prediction of Aircraft Response to Runway Roughness, AFWL-TR-73-109, Volume I and II, Air Force Weapons Laboratory, Kirtland AFB, New Mexico, September 1973.